Energy

Influence of operational parameters on the performance of Tesla turbines: experimental investigation of a small-scale turbine

André Luis Ribeiro Thomazoni[1], Conrado Ermel[1], Paulo Smith Schneider[1], Lara Werncke Vieira[1], Julian David Hunt[2], Sandro Barros Ferreira[3], Charles Rech[4], Vinicius Santorum Gouvêa[5]

Abstract

Tesla turbines can be employed as small-scale turbines to recover waste energy in several industrial applications. However, there is no consensus on the turbine efficiency as experimental studies show significantly lower values than those obtained by analytical and CFD approaches. The present work addresses that question by performing a systematic literature review (SLR) on Tesla turbines, comparing the efficiency values reported by experimental and simulation works. To validate the SLR findings an experimental small-scale air driven Tesla turbine was built. The Design of Experiments (DoE) methodology was applied to understand the effects of selected independent variables on the turbine output power and mechanical efficiency. Inlet air pressure, temperature, and rotational speed were chosen as controllable factors of a Central Composite Design applied to the prototype of < 1kW output power. The results indicate the average effect of 1 bar increase in the input pressure leads to an efficiency increase of 5%. In the SLR an average efficiency of 40% to 60% was reported by simulation works, while experimental essays reported maximum efficiencies of 20%. The experimental turbine analyzed in this paper presented a maximum efficiency of 14.2% ±0.4% at 3 barg and 4,000 rpm, agreeing with other experimental studies.

Tesla turbine; Design of experiments; Small-scale turbine; Systematic literature review

[1] Federal University of Rio Grande do Sul, Brazil
[2] International Institute for Applied Systems Analysis (IIASA), Austria
[3] IntelliSense.io, United Kingdom
[4] Federal University of Santa Maria, Brazil
[5] Pontifical Catholic University of Rio Grande do Sul, Brazil

- Literature review shows a lack of consensus regarding the TT maximum efficiency.
- The designed TT is limited to efficiencies below 20%
- Higher efficiency could be found for output power ≤ 1 kW and forward into sub-Watt scale.
- Is still to be proven that TT performance can be competitive concerning other turbine technologies.

1 Introduction

Tesla turbine, also known as multi-disc turbine, was patented by N. Tesla in 1913 [1]. Despite the little interest aroused since its invention, the Tesla turbine (TT) has recently become an object of study as presented in Figure 1.

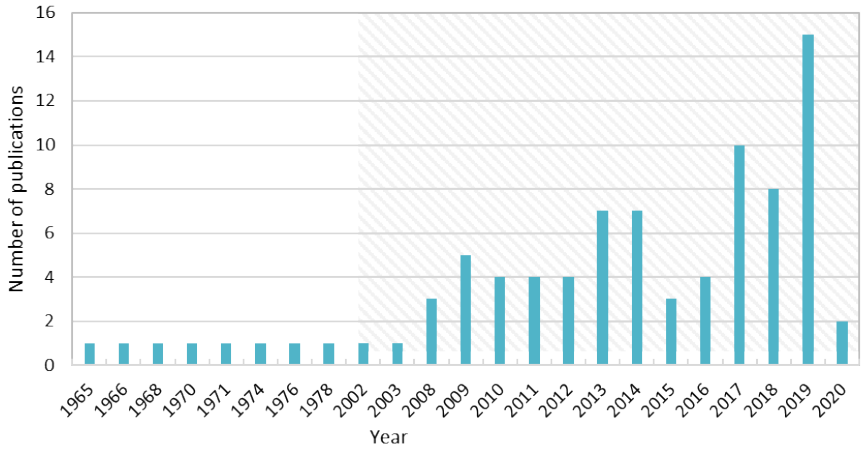

Figure 1 – Number of publications per year on Tesla turbine since 1964 (years without publications were suppressed).

More than 90% of the TT related papers were published in the 2000's and 2010's (hatched area). The little interest until the 2000's is due to equipment higher losses when studied as a turbine for large generation power plants (large scale) [2].

That recent increase in the number of studies is related to the demand for energy efficiency solutions, particularly those involving low power output levels. Results of pioneering works in the analysis of TT pointed to the potential use of this equipment as small-scale turbines ([3,4] [5]). This type of equipment can be seen as an alternative for diverse energy recovery projects, such as: (i) low output power ORC ([2], [6], [7], [8], [9]); (ii) energy harvesting ([10]; [11,12] [13]); and (iii) micro-cogeneration with low energy availability gases/streams ([14], [15], [16], [17], [18]).

The state of the art on TT research was assessed by performing a systematic literature review SLR, which comprised bibliometric and content analysis, including research and conference papers, available on Scopus® and Web of Science (WoS) databases, which are representative scientific databases in the engineering field [19,20]. The following query string was adopted: *ALL ("Tesla turbine*" OR "Boundary layer*

turbine" OR "Bladeless turbine*" OR "Multiple Dis* turbine*" OR "Viscous turbine*").* 301 documents were retrieved from Scopus and 65 from WoS. A content analysis was performed for the reduced set of 86 papers, selected after a filtering and preliminary reading process. The main findings are reported in this section, which also presents the research question of this work. The APPENDIX contains the complete bibliometric analysis and additional information of the content analysis.

Figure 2 presents the distribution of problem-solving approaches addressed by the 86 selected documents. Most of the works (45) concentrated on analytical tools to model the TT behavior, followed by experimental (39) and CFD (38) approaches. Two papers were presented as reviews [21,22].

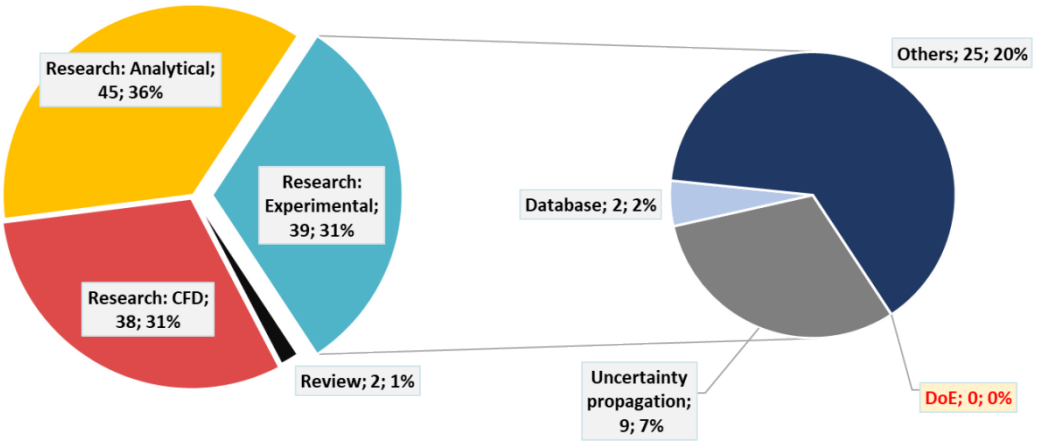

(a) (b)

Figure 2 – Type of studies on Tesla turbine: a) problem-solving approaches and b) quality analysis of experimental studies.

Although the majority of the papers are non-experimental (67%), it was found that the experimental ones were often used to validate new analytical and CFD solutions, especially the work reported by Rice [3], which is the most cited one (Figure A.2). Therefore, a deeper analysis of the experimental results was performed (Figure 2.b) to identify the composition of the available data based on the existence of: (i) uncertainty propagation analysis (9); (ii) a database that presents efficiency, power, mass flow rate and thermodynamics states at the inlet and outlet of the turbine (2); (iii) a statistical analysis, such as Design of Experiments DoE. It was found that most of

the presented studies (25) did not assess any uncertainty propagation analysis, and no one applied DoE concepts.

Efficiency and output power were used to characterize turbine behavior in most of the selected papers, as shown in the performance map in Figure 3.

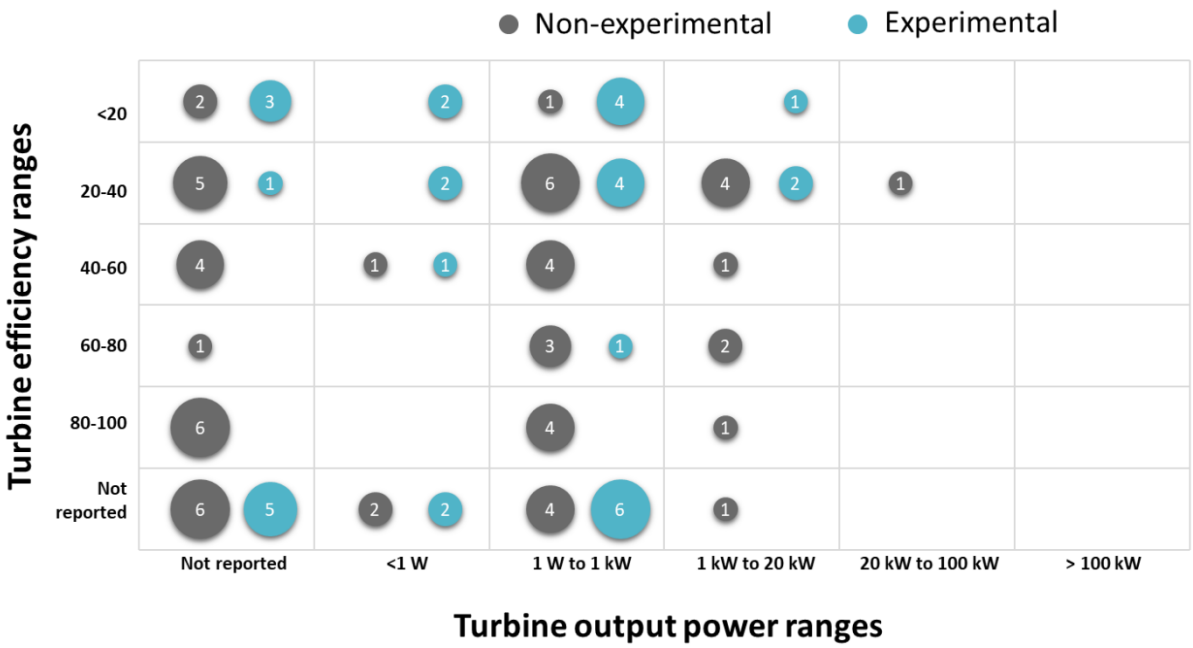

Figure 3 – Tesla turbine performance map (efficiency vs output power). Circle diameter indicates the number of papers on both power and efficiency; the circle color indicates the problem-solving approach. Reported results were filtered to consider a single contribution per paper (for efficiency and/or output power), by keeping their respective most relevant findings.

Results in Figure 3 show that 98% of the reported output power (59 of 60 values) was found below 20 kW. The highest experimental output power was reported by Rice [3], for a 4 kW bench equipment. A significant number of experimental works were developed on the sub-watt scale (10 of 60 reported values), but only a few CFD/analytical approaches were dedicated to that same range (3 of 60 values). These findings reinforce the application of TT as a small-scale turbine and point out the recent trend of its use as an energy harvesting device on the sub-watt scale.

Considering all reported data, TT efficiency is mostly found within the 20%-40% range (25 of the 67 values), followed by 13 values of efficiency lower than 20%. TT performance values are uncertain when it comes to defining the equipment's

maximum efficiency, especially when data from analytical or CFD approaches are to be compared with experiments. Experimental works concentrate the efficiency values in lower ranges with 10 values less than 20% and 9 values between 20%-40%. Efficiency values of non-experimental works indicate a more balanced distribution, with 16 values between 20%-40%, 11 values >80% and 10 values between 40%-60%. This data dispersion may explain the recent increase in the number of publications, as TT efficiency is not well understood yet.

Different definitions of efficiency can be found for TT. A quantitative analysis of the most applied definitions is shown in Figure 4.

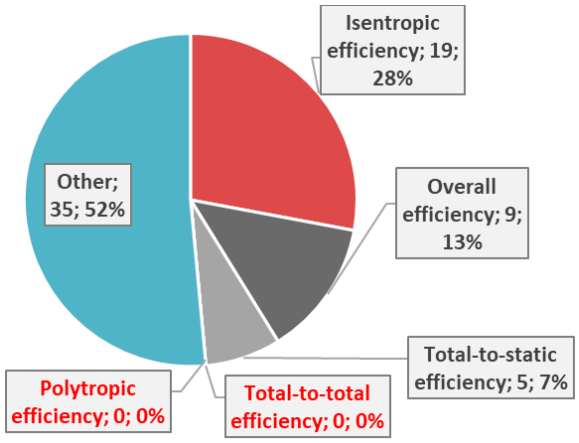

Figure 4 – Distribution of reported efficiency according to its physical definition.

The variety on the definition of the TT efficiency helps to understand why there is no agreement on its reported values. The majority of the selected papers (35 out of 69 reports) did not indicate the physical definition for efficiency. Sengupta & Guha [23] recommend caution when interpreting TT efficiency values due to the lack of a consensual definition, like the one proposed for gas turbines.

The maximum efficiency reported by experimental works varies significantly, and the lack of rigor in the experimental approaches may contribute to it. The SLR helped to identify the need for a more comprehensive approach to the problem. Therefore, the following research question was stated: How the Tesla turbine output power and efficiency are sensitive to its key parameters?

To answer the research question a 1 kW TT prototype was designed and built. A bench rig was also assembled to perform the assessment. A Design of Experiment DoE

planning was applied to understand how the independent key parameters affect the TT output power and mechanical efficiency, as also to produce a reliable database.

2 Tesla turbine description and key parameters

The effects of enthalpy and pressure changes on the working fluid in a TT can be compared with those of conventional turbomachinery, but the dynamic action principle differs from bladed turbines due to the constructive shape of its rotor (Figure 5).

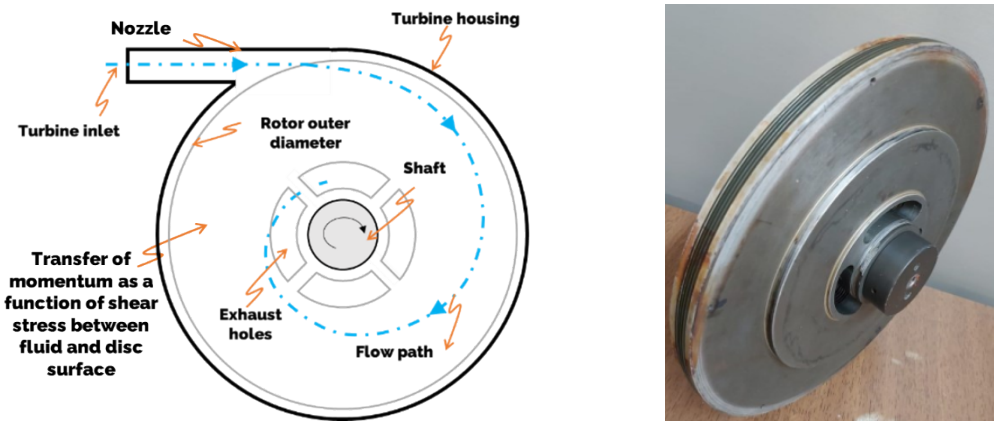

(a) (b)

Figure 5 – (a) TT schematic flow drawing; (b) TT manufactured rotor.

Pressurized inlet air flows through the turbine nozzle to be converted into kinetic energy, which is directed to the rotor. The rotor consists of a set of parallel concentric flat discs mounted on a shaft. The flow transfers its energy to the disc surfaces by friction, to finally exit the turbine through a channel at the rotor base. That configuration allows characterizing the Tesla turbine rotor as a radial inflow.

A comprehensive literature search was carried out to identify and classify the independent parameters that affect TT output power and efficiency, based on [22,24], and depicted in **Error! Reference source not found.**. The inner circle brings 5 key parameter categories, displayed in different colors, while the outer circle gathers the related information.

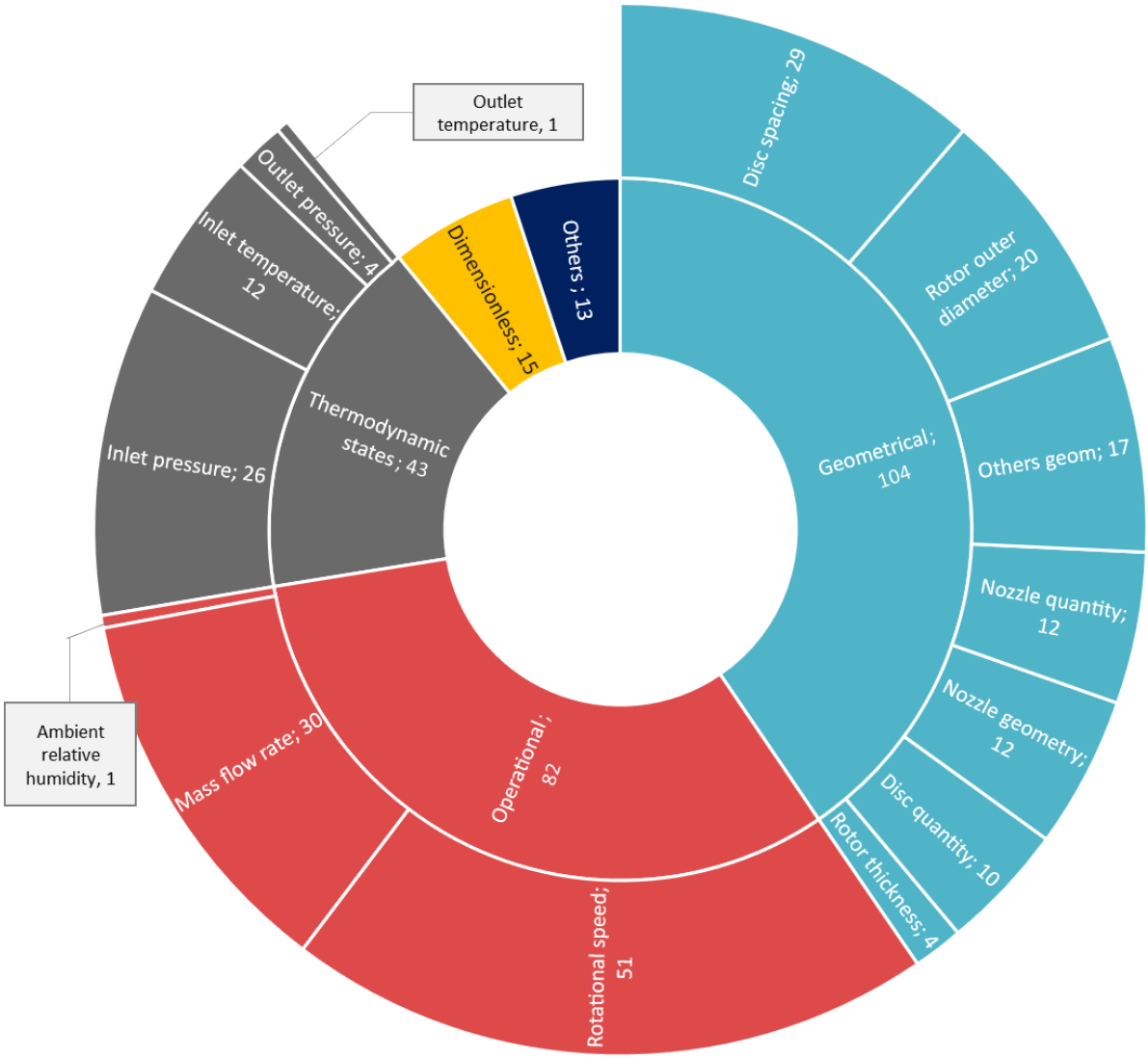

Figure 6 – Tesla turbine key parameters and their number of occurrences according to the SLR: parameter category (inner circle); parameter description (outer circle)

The geometrical category encompasses 7 parameters, with the highest occurrences for Disc Spacing [mm] (29) and Rotor Outer Diameter [mm] (20). The operational category presented three parameters, of which two parameters can be considered as main ones: Rotational Speed [rpm] (51) and Mass Flow Rate [kg/s] (30). The Thermodynamics category brought inlet pressure (26) as the most cited key parameter. The dimensionless key parameters were mainly reported in analytical approaches.

A summary of those key parameters and their influence on the output power and efficiency is following presented:

Rotational speed: the output power and efficiency behave non linearly in respect to the rotational speed, approximated by a 2nd order polynomial [4,11,32–41,23,42–44,25–31] for a fixed geometry and inlet conditions. Analytical works [23,43] reported higher output power when TT is designed to operate at high rotational speeds, but with low efficiencies. The highest experimental output power reported in the literature [3] was around 3 kW with rotation speed close to 18,000 rpm and efficiency of approximately 35%.

Mass flow rate (MFR): for a fixed rotational speed output power is directly coupled to MFR, as reported by [10,33,45–48]. These results may indicate that the greater the MFR, the higher the output power, however, some works reported an ideal MFR value that maximizes efficiency, and that changes in MFR (increase or decrease) will generate a loss in efficiency [12,31,47,49] [3,7,50,65,66]. Despite being an obvious finding, little is known about the mechanisms of TT loss of efficiency due to the increase in MFR.

Inlet flow pressure: a direct relation of output power in respect to the inlet flow pressure was reported by [4]. However, this increase in output power was noticed to be less intense than the one concerning the available energy, or the enthalpy drop across the turbine. That characteristic can explain the non-linear behavior of the turbine efficiency in respect to the inlet flow pressure, also corroborated by [3,38,44,71,72,51–53,57,62,63,67,69]). It is interesting to point out that the behavior observed due to the increase in inlet pressure is almost identical to that observed due to the increase in MFR.

Inlet flow temperature: Manfrida et al. [7] stated that it is expected a direct relation of output power to temperature levels, but with an opposite trend for efficiency, similar to the one of inlet flow pressure. On the other hand, [53] reported that the temperature rise should generate an increase in both output power and efficiency, similarly to the one expected from rising inlet flow pressure, but to a lesser degree. Few studies were dedicated to this key parameter.

Nozzle number: three trends were observed: (i) direct relation of efficiency and output power to the number of nozzles ([34,45,51,54]); (ii) the opposite [29,46,55]; (iii) no noticeable change [53]. Some authors proposed the “one-to-one” configuration [34,35,56], with nozzles with the same disc spacing and channel number that the ones found in the rotor stack, in opposition to the conventional nozzle configuration of “one-

to-many". Qi et al. [34] compared those two options and reported a better performance for the one-to-one configuration.

Rotor outer diameter: assessment was mostly performed through analytical and CFD approaches, and changes in rotor outer diameter influence both efficiency and output power [10,40,43,46,57–61]. The majority of the reported results indicate an increase in turbine output power for larger outer diameter [10,40,43,46,57–60]. Also, there is an ideal value of the outer diameter that maximizes the efficiency and is often expressed as a diameter ratio (inner diameter/ outer diameter). Talluri et. al, 2018, [43] which maximum efficiency of 35% for diameter ratio between 0.3 to 0.5. Guha & Sengupta, 2017, [58] found the maximum efficiency of 55% for diameter ratio within 0.52-0.7.

Disc number: few works on the influence of the number of discs on the TT performance were found, despite its relevance. Some of them stated that efficiency increased with the number of discs [10,34], while others reported the opposite [43]. Pfenniger et al. studied rotor stacks with 4, 7, and 11 discs, demonstrating that there is an ideal number of discs for which the efficiency is maximized, and further changes will negatively affect the TT efficiency.

Disc spacing: two trends in efficiency behavior were identified: (i) increasing the disc spacing leads to a decrease in both efficiency and output power [4,11,12,52]; (ii) there is an ideal disc spacing that maximizes efficiency, but changes around it can make efficiency to readily decrease [7,10,28,34,41,43,58,62,63]. Results from both experimental and CFD approaches diverged in respect to output power behavior. CFD works from [28,43,63] show that higher disc spacing leads to higher output power, which was countered by experimental works from [4,10]. That discrepancy may be explained by a possible non-consideration or underestimation of friction losses.

3 Experimental investigation

A small-scale prototype of a Tesla turbine, Figure 7, was built to be tested under atmospheric pressure exhaust. The turbine was assembled with a single convergent nozzle (rectangular with 30 mm^2 of outlet area), and six aluminum discs rotor to yield < 1 kW power output. Table 1 presents the detailed construction parameters.

Table 1 – Tesla turbine in details (For the turbine design, except where indicated, all dimensions were manufactured according to NBR ISO 2768-1 [64], medium class).

Rotor outer diam.	**Rotor inner diam.**	**Discs exhaust area**	**Disc thickness**	**Discs quant.**	**Disc spacing**	**Casing - rotor gap**	**Nozzle quantity**	**Nozzle angle - tangent**	**Working fluid**	**Max. tested rotational speed**
(mm)	(mm)	(mm^2)	(mm)	un.	(mm)	(mm)	un.	°		(rpm)
300	100	3855	1	6	1	0.5	1	5	Air	6,000

The prototype was tested in a bench to map dependent variables like torque, output power, mass flow rate and efficiency. Information about the test bench arrangement and instrumentation is presented in Figure A.9 and Table A.2.

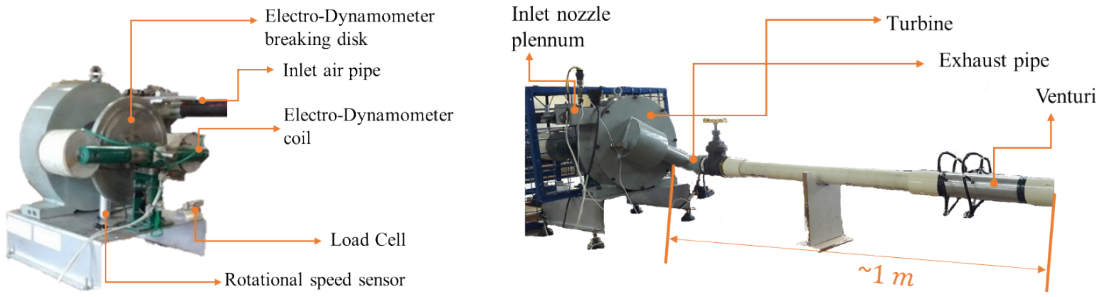

(a) (b)

Figure 7 – Tesla turbine test bench: (a) Foucault dynamometer; (b) Flow discharge and measurement.

The adopted experimental approach to characterize the TT and answer the research question of this paper was the Central Composite Design CCD, which is a fractional factorial design used in the Response Surface Methodology RSM suitable to identify nonlinear behavior [65–68]. The experiment was designed as a face-centered

design (orthogonal) with an $\alpha - value$ equal to 1, minimizing the number of levels, leading to more accurate estimations at the center of the domain [68]. The independent variables inlet air pressure, inlet air temperature and rotational speed were set for 3 levels, generating 20 combinations called experimental cells, described in Figure 8. The confidence level of 95% and statistical power of 80% required the performing of two experiment replicates. The inlet air pressure was controlled by the valve (PCV01), the temperature by the Heater connected to a dedicated CLP, and the rotor speed with the Electrodynamometer.

		Inlet pressure		
	Level	2 barg	2.5 barg	3 barg
Rotational speed (rpm)	2000	1x(30 °C); 1x(50 °C)	1x(40 °C)	1x(30 °C); 1x(50 °C)
	4000	1x(40 °C)	1x(30°C); 6x(40 °C); 1x(50°C)	1x(40 °C)
	6000	1x(30 °C); 1x(50 °C)	1x(40 °C)	1x(30 °C); 1x(50 °C)

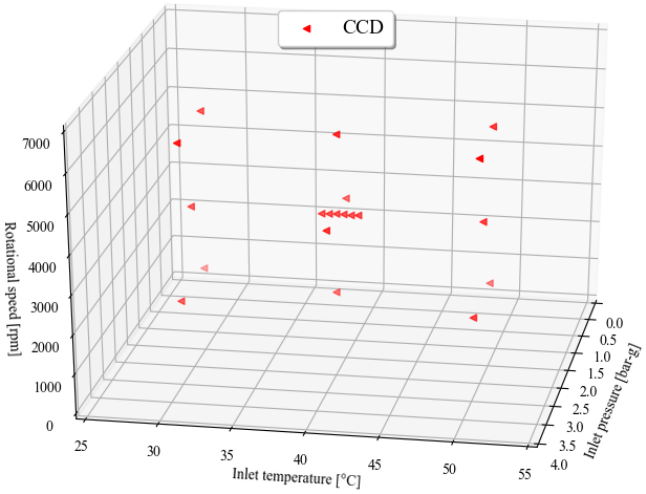

Figure 8 – CCD experiment level combination for a single replicate and three-dimensional domain of the independent variables.

For each experimental cell, the four dependent variables were calculated. Their equations are presented as follows. The turbine mass flow rate $\dot{m}_V$ (kg/s) was obtained from Eq. (3.1) [69]:

$$\dot{m}_V = \frac{(FC)C_{DV}\varepsilon_V \frac{\pi}{4} d_{iV}^2 \sqrt{2\,\Delta P_V\,\rho_V}}{\sqrt{1-\beta_V^4}}, \tag{3.1}$$

with C_{DV} the Venturi dimensionless discharge coefficient, 0.995, ε_V expansibility factor defined in [69], d_{iV} is the inner diameter of the Venturi Throat, m, β_V is the inlet-throat inner diameter ratio of the Venturi, ΔP_V is the differential pressure from inlet-throat of the Venturi, Pa, FC is the correction factor 1.0275, and ρ_V is the calculated air density.

The turbine torque T_{turb} (Nm) was calculated by Eq.(3.2):

$$T_{turb} = F_{LC} d_{ele}, \tag{3.2}$$

with F_{LC} the load cell force, *N*, and d_{ele} the lever length (0.2 m ± 0.001 m).

The turbine output power $\dot{W}_{turb}$ (W) was obtained from Eq. (3.3):

$$\dot{W}_{turb} = T_{turb} \Omega, \tag{3.3}$$

with Ω the turbine angular velocity, rad/s

The Tesla turbine mechanical efficiency is η_{m-turb} (dimensionless) was calculated from Eq. (3.4):

$$\eta_{m-turb} = \frac{\dot{W}_{turb}}{\dot{m}_V (h_{01} - h_{02s})}, \tag{3.4}$$

with h_{01} the stagnation enthalpy at turbine inlet, kJ/kg, e h_{02s} stagnation isentropic enthalpy at the turbine outlet, kJ/kg.

Expanded uncertainties of dependent variables were expressed as recommended by GUM [70], for a 95.45% confidence level (Table 2).

Table 2 – Summary of expanded uncertainty for the dependent and independent variables (confidence level of 95.45%).

Dependent variable	Expanded uncertainty	Unit	Independent variable	Expanded uncertainty	Unit
$Inlet\ Pres.$	± 0.05	bar	T_{turb}	± 0.1	(Nm)
$Rotational\ speed$	± 4.7	rpm	$\dot{W}_{turb}$	± 6.5	(W)
$Inlet\ Temp$	± 0.6	° C	$\dot{m}_V$	± 0.0005	(kg/s)
			η_{m-turb}	± 0.4	(%)

The essays sequence was randomized with the aid of Minitab 18 and is presented in Table A.3. Each experimental data cell was acquired 3 minutes after turbine stabilization with an 0.1 s acquisition rate. Data were filtered for outliers [71] to generate a database with the average value of independent and dependent variables.

The complete set of consolidated values is available in Table A.3. The last step concerns the statistical analysis to identify the parameter influence and interactions; to rank the independent variable importance and to build regression equations that define the turbine dependent variable behaviors.

4 Test results and discussion

As part of the DoE analysis, the ANOVA (Analysis of Variance) was performed with data from Table A.3 for each of the four dependent variables, resulting in the determination of parameters such as the sum of squares, degree of freedom, mean sum of squares, F-statistic, and p-values. With these values, it is possible to apply statistical tests and determine and rank the significant(s) independent variable(s). Once the ANOVA was performed, the normal probability plots were checked to verify the assumption that the errors are normally distributed, with constant variance and independence [67]. Figure 9 depicts the normal probability plots for each dependent variable and shows that the normality assumption is checked for the measured data.

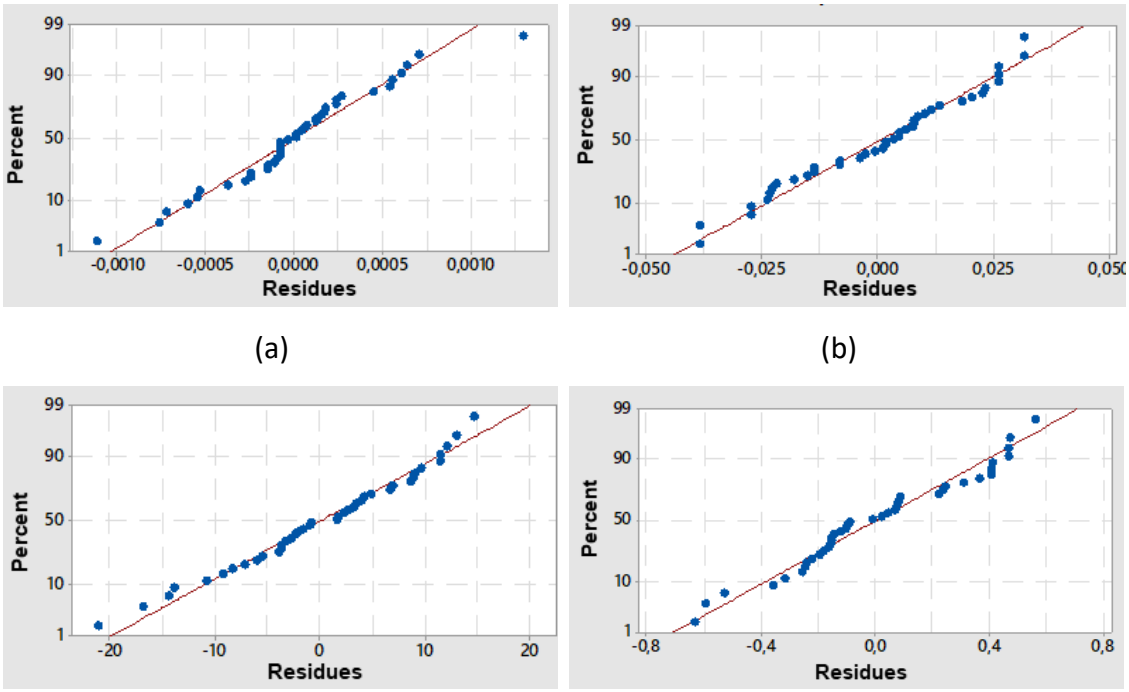

Figure 9 – Normal probability plot: (a) $\dot{m}_V$; (b) T_{turb}; (c) $\dot{W}_{turb}$; and (d) η_{m-turb}.

The statistically significant effects and interactions for the independent variable range allow for ranking the parameters by the most significant one to the least in the studied range. These results are summarized in Table 3, which is elaborated by

observation of the Pareto chart for standardized effects and normal plot for standardized effects, both obtained with Minitab 18.

Table 3– Summary of effects and interactions for 95% of confidence: (↑ ≡ rising effect; ↓ ≡ lowering effect); the number indicates the standardized effects from Pareto a with statistical significance limit = 2.03.

Indep. / Dep.	Inlet pressure	Inlet temperature	Rotational Speed	Interactions
$\dot{m}_V$	– **Linear (↑;31,4)**	– Linear (↓;4,9)	----------	----------
T_{turb}	– Linear (↑; 51,8) – Quad. (↓, 4,1)	----------	– **Linear (↓;77,9)** – Quad. (↓;12)*	– Angular speed.* Press (↓;10,5)
$\dot{W}_{turb}$	– **Linear (↑; 43,9**) – Quad. (↓; 3,1)	----------	– Linear (↓; 12,6) – Quad. (↓; 32,1)	– Angular speed* Press (↑; 11,5)
η_{m-turb}	– Linear (↑; 29,8) – Quad. (↓; 7,25)	----------	– Linear (↓; 18,6) – **Quad. (↓; 44,9)**	– Angular speed* Press (↑; 17,3)

The most recurrent effect was the pressure linear, which presented a pattern of increment behavior in the dependent variables as the inlet pressure is increased. This linear effect also is the most relevant for $\dot{m}_V$ and $\dot{W}_{turb}$. For the η_{m-turb} the quadratic effects rotational speed is the most relevant, decreasing the efficiency value. It was found that the pressure quadratic effect decreases the values of the dependent variables, which may be related to the effects of turbine efficiency losses.

The rotational speed*pressure interaction increased the effects on $\dot{W}_{turb}$ and η_{m-turb}, however, for torque, it showed a behavior of decreasing the perceived effect. The temperature effect is statistically relevant only for $\dot{m}_V$, decreasing its value as the inlet temperature increases.

In Figure 10 it is possible to graphically analyze the effects summarized in Table 3. The figures were obtained from the Minitab 18 software and only the main effects and interactions that are statistically significant were plotted for each of the four dependent variables.

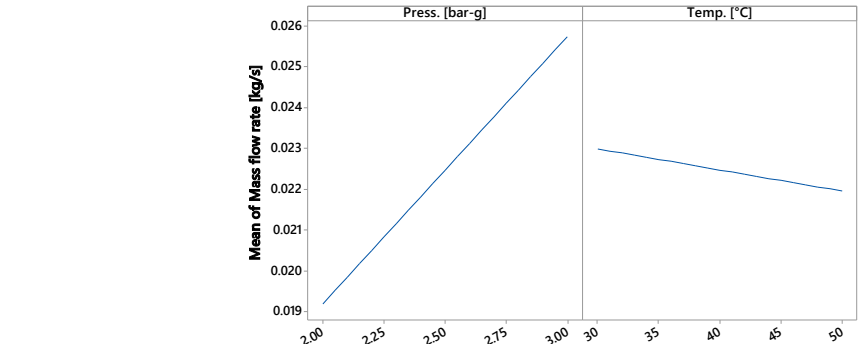

(a)

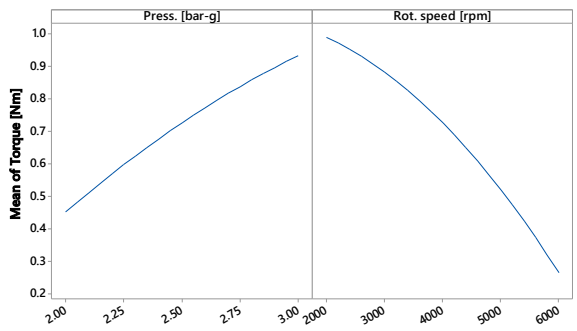

(b)

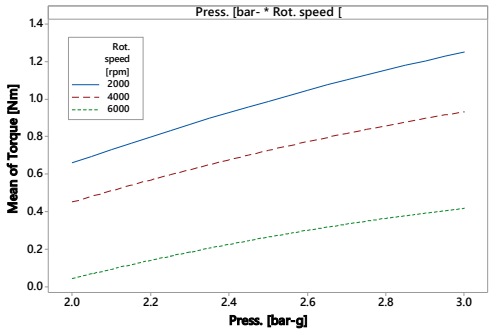

(c)

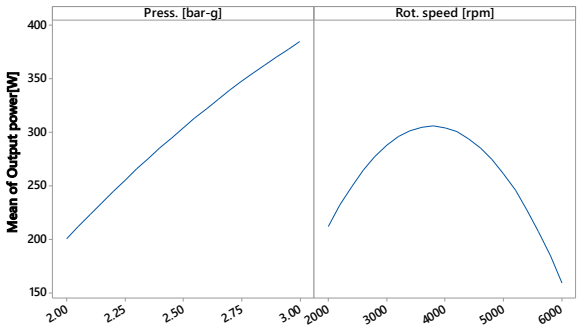

(d)

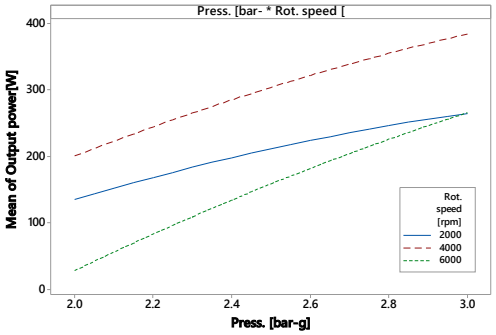

(e)

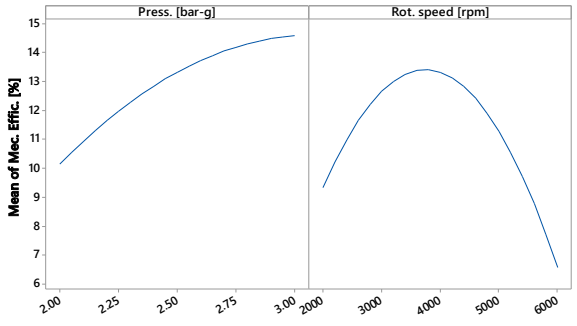

(f)

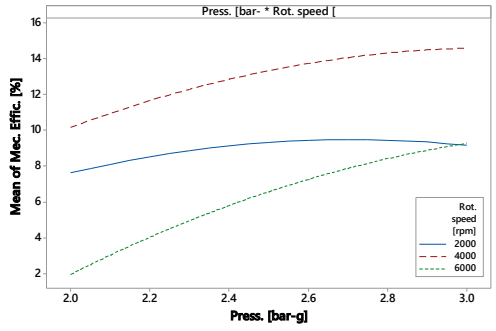

(g)

Figure 10 – Main effects and interaction plots with statistical significance limit = 2,03: (a) main effects – $\dot{m}_V$; (b) main effects – T_{turb}; (c) interactions effects – T_{turb}; (d) main

effects – $\dot{W}_{turb}$; (e) interactions – $\dot{W}_{turb}$; (f) main effects – η_{m-turb}; (g) interactions – η_{m-turb}.

The turbine mass flow rate $\dot{m}_V$ increased 34% with 1 bar of inlet pressure increase, on average, while increasing inlet temperature in 20 °C decreased 4% of its value (Figure 10(a)). Average results for turbine torque T_{turb} indicated that 1 bar increase in inlet pressure enhances 2.1 times its values, whereas the effects of a rise in rotational speed decreased it 4 times (Figure 10(b)). The interaction effects of air pressure and rotational speed (Figure 10(c)) on T_{turb} indicated that the latter became less important for higher angular velocity values.

Figure 10(d) shows that the turbine output power $\dot{W}_{turb}$ increased by the ratio of 2 per bar, on average, with a 150 W overall increase. The effect of rotational speed is mainly quadratic with the maximum value within the studied range and approximately equal to 4.000 rpm. The interaction effect in Figure 10(e) is more evident due to the crossing lines, which indicates that the effect caused by the pressure increase leads to higher $\dot{W}_{turb}$ at higher rotations and drops the intensity for lower rotational speeds.

The turbine efficiency η_{m-turb} directly responded to the increase in the inlet air pressure (Figure 10 (f)), with the ratio of 1.5/bar, adding almost 5 percentage points. A maximum value for η_{m-turb} should be reached by expanding the inlet pressure beyond 3 barg. The interaction in Figure 10 (g) presented crossing lines pointing out that higher values of η_{m-turb} should be obtained with higher values of rotational speed.

Table 4 presents the surrogate model for the four dependent variables, whose comparison with measured data is detailed in the APPENDIX (Table A.4). Also, in Table 4 the results of the coefficient of determination R^2 are presented. The R^2 is applied as the prediction quality metric of the obtained surrogate models with CCD-FCC. The R^2 values show a strong relationship between the effects observed in the dependent variables as a function of the changes imposed on the values of the independent variables. The R^2 for η_{m-turb} is 99.32%, which indicates that only a variation of 0.68% is not explained by the change in the dependent variables of the surrogate model.

Table 4 – Surrogate model and quality metrics of the turbine dependent variables: mass flow rate $\dot{m}_V$, (kg/s), torque T_{turb}, (Nm), output power $\dot{W}_{turb}$, (W), and mechanical efficiency η_{m-turb}, dimensionless, (input data in barg, °C and rpm).

Equation		S_m	R^2	S_{aj}^2	S_{pd}^2
$\dot{m}_V = 0.008175 + 0.006540 * \text{Pressure} - 0.000051 * \text{Temperature}$	(4.1)	0.0005 kg/s	96.65%	96.37%	95.65%
$T_{turb} = -1.5463 + 1.3808 * \text{Pressure} + 0.0001531 * \text{Rotational speed} - 0.1363\ (\text{Pressure})^2 - 0.0000000248 * (\text{Rotational speed})^2 - 0.00005438 * \text{Pressure} * \text{Rotational speed}$	(4.2)	0.02 Nm	99.64%	99.58%	99.50%
$\dot{P}_{turb} = -599.6 + 308.3 * \text{Pressure} + 0.15738 * \text{Rotati} - 46.5\ (Pressure)^2 - 0.00002973 * (\text{Rotational speed} 0.02696 * \text{Pressure} * \text{Rotational speed}$	(4.3)	9 W	99.19%	99.04%	98.83%
$\eta_{mec-turb} = -25.84 + 17.7 * \text{Pressure} + 0.006448 * \text{Rotational speed} - 3.81\ (\text{Pressure})^2 - 0.000001335 * (\text{Rotational speed})^2 + 0.001433 * \text{Pressure} * \text{Rotational speed}$	(4.4)	0.30%	99.32%	99.19%	99.01%

The dispersion between measured and predicted data is given by the surrogate model standard deviation (S_m). which presented smaller values than the observed average effects. showing that the perceived effects (Figure 10) are larger than the model standard deviation. The surrogate model values for the statistical metric S_{aj}^2 are similar to their respective R^2 and above 90%. indicating that no additional predictor variables are required. The comparison of the predicted coefficient of determination S_{pd}^2 with the respective R^2 demonstrates that there is no excess of adjustment for any of the surrogate models.

The map of the Tesla turbine performance is depicted in Figure 11 for a confidence level of 95%.

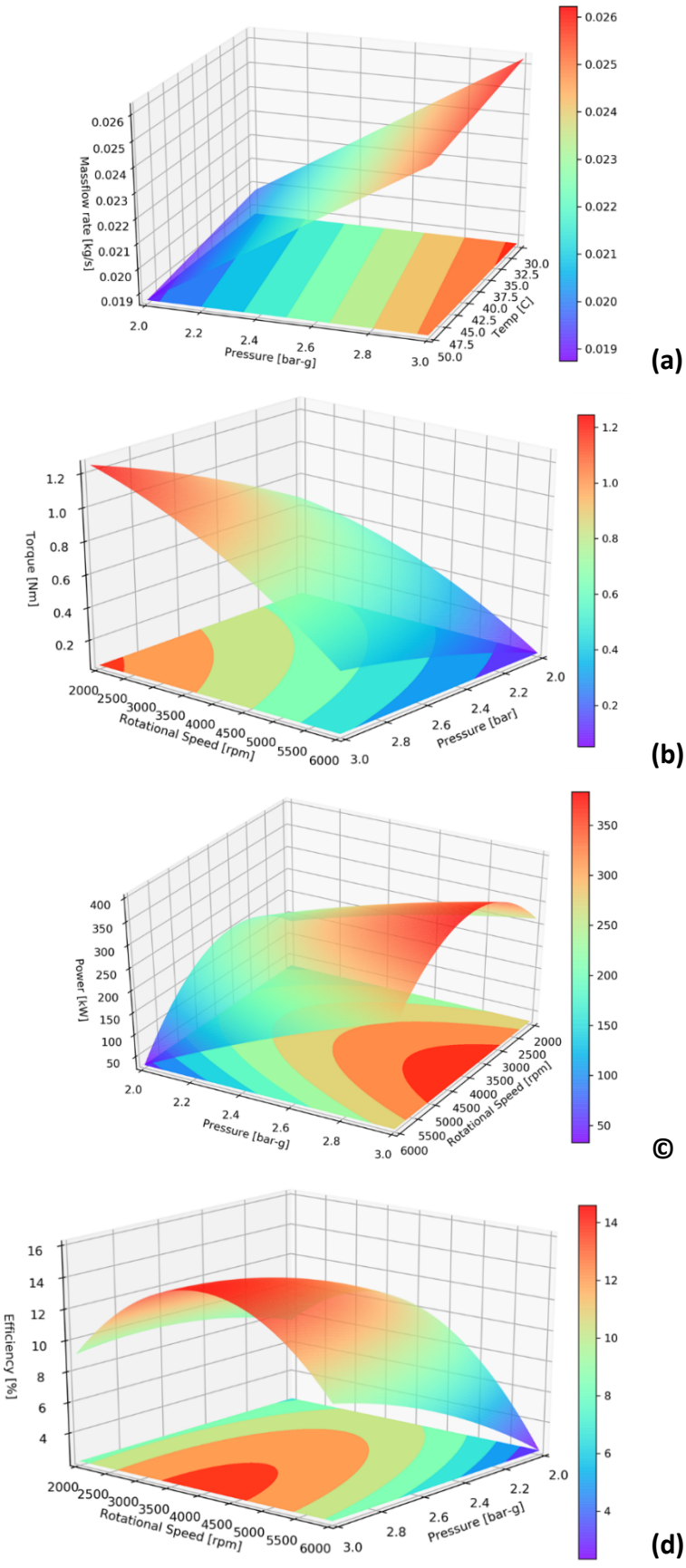

Figure 11 – Tesla turbine performance surface and contour plots: (a) $\dot{m}_V$; (b) T_{turb}; (c) $\dot{W}_{turb}$; (d) η_{m-turb}.

A quadratic behavior is observed for T_{turb}. $\dot{W}_{turb}$ and η_{m-turb} as a function of the pair of independent inputs rotational speed and inlet pressure. The higher predicted value for $\eta_{m-turb}$was 14.5% @ 3 bar-g and 4.020 rpm. which is close to the maximum measured η_{m-turb} of 14.2% ± 0.4% @ 3 bar-g e 4.000 rpm. The predicted value for $\dot{W}_{turb}$ was 384 W. and its maximum measured value was 394.0 W ± 6.5 W @ 3 bar-g and 4.000 rpm. The $\dot{m}_V$ presented a linear behavior. mostly due to the inlet pressure. indicating the expected behavior of the convergent nozzle in a choked flow condition [72–74].

5 Conclusions

The DoE approach allowed us to statistically assess experimental results and define the sensitivity of the dependent variables regard to the air inlet pressure. air inlet temperature e rotational speed. The independent variables inlet air pressure and rotor rotational speed were identified as the most influent in respect to the Tesla turbine performance. with the coefficient of determination R^2 equal or greater than 95% for the surrogate models of mass flow rate $\dot{m}_V$. torque T_{turb}. output power $\dot{W}_{turb}$. and mechanical efficiency η_{m-turb}.

For the increase of 1 bar in inlet pressure. $\dot{W}_{turb}$ enhanced almost 2 times and the obtained behavior indicates that a further increase in this factor should lead to even higher values for output power at higher values of rotational speed. For η_{m-turb} the change in inlet pressure led to an increase in almost 5 percentage points in its value. however. it is possible to observe that a practical limit is close to being obtained if the inlet pressure is further increased. This behavior could be related to a probable increase in loss effects inside the turbine for higher inlet pressure. despite the rising trend in the output power due to inlet pressure increase.

Results for $\dot{m}_V$ indicate that the turbine presented a choked flow behavior due to an under expanded condition at the nozzle. and the statistically significant factors are inlet pressure and inlet temperature. It is interesting to point out that results for $\dot{m}_V$ present a linear relationship with inlet pressure (1:1). since the increase of 34% in inlet pressure absolute value resulted in the same increase in $\dot{m}_V$. Increasing the inlet

temperature in 20°C caused the mass flow rate to decrease 4%. For the designed convergent nozzle configuration. further increase in temperature values should lead to lower $\dot{m}_V$. and. probably. should generate a negative effect on power output and mechanical efficiency.

The combination of 3 bar-g and 4.000 rpm. results in the higher predicted value for η_{m-turb} and $\dot{W}_{turb}$. The turbine efficiency was equal to 14.5% and close to the measured value of 14.2% ± 0.4%. The predicted $\dot{W}_{turb}$ was 384 W and the maximum measured value was 394.0 W ± 6.5 W. The inlet temperature in the range of levels that were studied did not have a statistically significant impact on mechanical efficiency.

The presented DoE approach granted the definition of practical limits for mechanical efficiency in the TT prototype and the behavior of interaction among the statistically significant factors. This allowed defining that the designed TT is limited to efficiencies below 20% and further changes in the independent variable values should not modify the maximum efficiency significantly. Thus. further work should pursuit the improvement of mechanical efficiency by studying the nature of the losses. as also the effects of changes in geometrical turbine characteristics.

6 Acknowledgments

Thomazoni, Vieira and Ermel acknowledge the financial support from CNPq (Conselho Nacional de Desenvolvimento Científico e Tecnológico) and CAPES (Coordenação de Aperfeiçoamento de Pessoal de Nível Superior) for their PhD grant. Schneider acknowledges CNPq for his research grant (PQ301619/2019-0).

BIBLIOGRAPHY

[1] Tesla N. TESLA TURBINE. 1061142, 1913.

[2] Ciappi L, Fiaschi D, Niknam PH, Talluri L. Computational investigation of the flow inside a Tesla turbine rotor. Energy 2019;173:207–17. https://doi.org/10.1016/j.energy.2019.01.158.

[3] Rice W. An analytical and experimental investigation of multiple-disk turbines. J Eng Power 1965;1:29–36. https://doi.org/10.1115/1.3678134.

[4] Beans EW. Investigation into the Performance Characteristics of a Friction Turbine. J Spacecr Rockets 1966;3:131–4.

[5] Trumars CR, Rice W, Jankowski DF. Laminar throughflow of quality steam between corotating disks. 1976.

[6] Manfrida G, Pacini L, Talluri L. A revised Tesla Turbine Concept for ORC applications. Energy 2018;158:33–40. https://doi.org/10.1016/j.energy.2018.05.181.

[7] Manfrida G, Pacini L, Talluri L. An upgraded Tesla turbine concept for ORC applications. Energy 2018;158:33–40. https://doi.org/10.1016/j.energy.2018.05.181.

[8] Song J, Gu C wei, Li X song. Performance estimation of Tesla turbine applied in small scale Organic Rankine Cycle (ORC) system. Appl Therm Eng 2017;110:318–26. https://doi.org/10.1016/j.applthermaleng.2016.08.168.

[9] Al Jubori A, Daabo A, Al-Dadah RK, Mahmoud S, Ennil AB. Development of micro-scale axial and radial turbines for low-temperature heat source driven organic Rankine cycle. Energy Convers Manag 2016;130:141–55. https://doi.org/10.1016/j.enconman.2016.10.043.

[10] Zhao D, Ji C, Teo C, Li S. Performance of small-scale bladeless electromagnetic energy harvesters driven by water or air. Energy 2014;74:99–108. https://doi.org/10.1016/j.energy.2014.04.004.

[11] Romanin V, Krishnan VG, Carey VP, Maharbiz MM. Experimental and analytical study of sub-watt scale tesla turbine performance. ASME Int Mech Eng Congr Expo Proc 2012;7:1005–14. https://doi.org/10.1115/IMECE2012-89675.

[12] Krishnan VG, Romanin V, Carey VP, Maharbiz MM. Design and scaling of

microscale Tesla turbines. J Micromechanics Microengineering 2013;23. https://doi.org/10.1088/0960-1317/23/12/125001.

[13] Mutsuda H, Rahmawati S, Taniguchi N, Nakashima T, Doi Y. Harvesting ocean energy with a small-scale tidal-current turbine and fish aggregating device in the Indonesian Archipelagos. Sustain Energy Technol Assessments 2019;35:160–71. https://doi.org/10.1016/j.seta.2019.07.001.

[14] Kim CK, Yoon JY. Performance analysis of bladeless jet propulsion micro-steam turbine for micro-CHP (combined heat and power) systems utilizing low-grade heat sources. Energy 2016;101:411–20. https://doi.org/10.1016/j.energy.2016.01.070.

[15] Ribeiro Thomazoni AL, Schneider PS, Tuo J, Vidoza Guillen JA, Ge Q, Boa Souza TF. Performance assessment of an alternative for energy efficiency in saturated steam systems. ECOS 2019 - Proc. 32nd Int. Conf. Effic. Cost, Optim. Simul. Environ. Impact Energy Syst., 2019, p. 2091–103.

[16] Włodarski W. Experimental investigations and simulations of the microturbine unit with permanent magnet generator. Energy 2018;158:59–71. https://doi.org/10.1016/j.energy.2018.05.199.

[17] Streit P, Popp T, Weiß AP. Simulation and analysis of the performance map of a micro-ORC-turbine - Comparison with measurements. AIP Conf Proc 2019;2189. https://doi.org/10.1063/1.5138634.

[18] Weiß AP, Popp T, Müller J, Hauer J, Brüggemann D, Preißinger M. Experimental characterization and comparison of an axial and a cantilever micro-turbine for small-scale Organic Rankine Cycle. Appl Therm Eng 2018;140:235–44. https://doi.org/10.1016/j.applthermaleng.2018.05.033.

[19] Ermel APC, Lacerda DP, Morandi MIWM, Gauss L. Literature Reviews: Modern Methods for Investigating Scientific and Technological Knowledge 2021:204. https://doi.org/10.1007/978-3-030-75722-9.

[20] Tarragona J, Fernández C, Cabeza LF, de Gracia A. Economic evaluation of a hybrid heating system in different climate zones based on model predictive control. Energy Convers Manag 2020;221:113205. https://doi.org/10.1016/j.enconman.2020.113205.

[21] Shah V, Dhokai S. Tesla Turbine Experiment. Int J Sci Res 2017;6:113–6.

https://doi.org/10.21275/art20175154.

[22] Zuber M, Ramesh A, Bansal D. The Tesla Turbine - A comprehensive review. J Adv Res Fluid Mech Therm Sci 2019;62:122–37.

[23] Sengupta S, Guha A. A theory of Tesla disc turbines. Proc Inst Mech Eng Part A J Power Energy 2012;226:650–63. https://doi.org/10.1177/0957650912446402.

[24] Rice W. Tesla turbomachinery. IV Int. Nikola Tesla Symp., 1991, p. 1–12.

[25] Guha A, Sengupta S. Similitude and scaling laws for the rotating flow between concentric discs. Proc Inst Mech Eng Part A J Power Energy 2014;228:429–39. https://doi.org/10.1177/0957650914523947.

[26] Guha A, Sengupta S. The fluid dynamics of the rotating flow in a Tesla disc turbine. Eur J Mech B/Fluids 2013;37:112–23. https://doi.org/10.1016/j.euromechflu.2012.08.001.

[27] Ji F, Bao Y, Zhou Y, Du F, Zhu H, Zhao S, et al. Investigation on performance and implementation of Tesla turbine in engine waste heat recovery. Energy Convers Manag 2019;179:326–38. https://doi.org/10.1016/j.enconman.2018.10.071.

[28] Klingl S, Lecheler S, Pfitzner M. Experimental, numerical and theoretical investigations of Tesla turbines. E3S Web Conf 2019;113:1–6. https://doi.org/10.1051/e3sconf/201911303003.

[29] Krishnan VG, Zohora I, Maharbiz MM. a Micro Tesla Turbine for Power Generation From Low Pressure Heads and evaporative driven flows. Am Soc Mech Eng 2011;013705:2–3. https://doi.org/10.1109/TRANSDUCERS.2011.5969878.

[30] Lemma E, Deam RT, Toncich D, Collins R. Characterisation of a small viscous flow turbine. Exp Therm Fluid Sci 2008;33:96–105. https://doi.org/10.1016/j.expthermflusci.2008.07.009.

[31] Lezsovits F. Decentralized energy supply possibilities based on biomass. Period Polytech Mech Eng 2003;47:151–68.

[32] Li R, Wang H, Yao E, Li M, Nan W. Experimental study on bladeless turbine using incompressible working medium. Adv Mech Eng 2017;9:1–12. https://doi.org/10.1177/1687814016686935.

[33] Pfenniger A, Vogel R, Koch VM, Jonsson M. Performance Analysis of a Miniature Turbine Generator for Intracorporeal Energy Harvesting. Artif Organs 2014;38. https://doi.org/10.1111/aor.12279.

[34] Qi W, Deng Q, Jiang Y, Yuan Q, Feng Z. Disc thickness and spacing distance impacts on flow characteristics of multichannel tesla turbines. Energies 2018;12. https://doi.org/10.3390/en12010044.

[35] Qi W, Deng Q, Jiang Y, Yuan Q, Feng Z. Aerodynamic performance and flow characteristics analysis of Tesla turbines with different nozzle and outlet geometries. Proc Inst Mech Eng Part A J Power Energy 2018;233:358–78. https://doi.org/10.1177/0957650918785312.

[36] Rusin K, Wróblewski W, Strozik M. Experimental and numerical investigations of Tesla turbine. J Phys Conf Ser 2018;1101. https://doi.org/10.1088/1742-6596/1101/1/012029.

[37] Rusin, Wróblewski, Rulik. The evaluation of numerical methods for determining the efficiency of Tesla turbine operation. J Mech Sci Technol 2018;32:5711–21. https://doi.org/10.1007/s12206-018-1118-4.

[38] Rusin K, Wróblewski W, Strozik M. Comparison of methods for the determination of tesla turbine performance. J Theor Appl Mech 2019;57:563–75. https://doi.org/10.15632/jtam-pl/109602.

[39] Schosser C, Lecheler S, Pfitzner M. A Test Rig for the Investigation of the Performance and Flow Field of Tesla Friction Turbines. Proc ASME Turbo Expo 2014 Turbine Tech Conf Expo 2014:1–11.

[40] Schosser C, Lecheler S, Pfitzner M. Analytical and numerical solutions of the rotor flow in tesla turbines. Period Polytech Mech Eng 2017;61:12–22. https://doi.org/10.3311/PPme.9000.

[41] Shaw D, Liu FT, Yu JJ. Experiment of a tesla engine for wind energy capture. Appl Mech Mater 2013;284–287:1051–6. https://doi.org/10.4028/www.scientific.net/AMM.284-287.1051.

[42] Song J, Ren X dong, Li X song, Gu C wei, Zhang M ming. One-dimensional model analysis and performance assessment of Tesla turbine. Appl Therm Eng 2018;134:546–54. https://doi.org/10.1016/j.applthermaleng.2018.02.019.

[43] Talluri L, Fiaschi D, Neri G, Ciappi L. Design and optimization of a Tesla turbine for ORC applications. Appl Energy 2018;226:300–19. https://doi.org/10.1016/j.apenergy.2018.05.057.

[44] Talluri L, Dumont O, Manfrida G, Lemort V, Fiaschi D. Experimental investigation

of an Organic Rankine Cycle Tesla turbine working with R1233zd(E). Appl Therm Eng 2020;174:115293. https://doi.org/10.1016/j.applthermaleng.2020.115293.

[45] Lampart P, Kosowski K, Piwowarski M, Jędrzejewski L. Design analysis of Tesla micro-turbine operating on a low-boiling medium. Polish Marit Res 2009;16:28–33. https://doi.org/10.2478/v10012-008-0041-5.

[46] Lampart P, Jedrzejewski Ł. Investigations of Aerodynamics of Tesla bladeless microturbines. J Theor Appl Mech 2011;49:477–99.

[47] Scafidi D, Roncallo F, Traverso A, Ferretti G, Pasta M, Pavan M, et al. Micro-turbine applied to seismology: Towards a power supply safe from lightning. E3S Web Conf 2019;113:3–6. https://doi.org/10.1051/e3sconf/201911303004.

[48] Borate HP, Misal ND. An effect of spacing and surface finish on the performance of bladeless turbine. ASME 2012 Gas Turbine India Conf GTINDIA 2012 2012:165–71. https://doi.org/10.1115/GTINDIA2012-9623.

[49] Romanin V, Carey VP, Norwood Z. Strategies for performance enhancement of Tesla turbines for combined heat and power applications. Proc. ASME 2010 4th Int. Conf. Energy Sustain., 2010, p. 1–8.

[50] Deam RT, Lemma E, Mace B, Collins R. On scaling down turbines to millimeter size. J Eng Gas Turbines Power 2008;130:1–9. https://doi.org/10.1115/1.2938516.

[51] Deng Q, Qi W, Feng Z. Improvement of a Theoretical Analysis Method for Tesla Turbines. Proc. ASME Turbo Expo 2013 Turbine Tech. Conf. Expo., 2013, p. 1–14. https://doi.org/10.1115/gt2013-95425.

[52] Hasan AM. Investigating the possibility of using a tesla turbine as a drive unit for an automotive air-conditioning compressor using CFD modeling. ASHRAE Conf 2016;122:146–58.

[53] Patel N, Schmidt DD. BIOMASS BOUNDARY LAYER TURBINE POWER SYSTEM. Proc. Int. Jt. Power Gener. Conf. 2002, 2002, p. 1–4.

[54] Kamran MA, Manzoor S. Effect of nozzle angle, turbine inlets and mass flow rate on the performance of a bladeless turbine. Proc Inst Mech Eng Part A J Power Energy 2019;234:1101–7. https://doi.org/10.1177/0957650919893539.

[55] Ji F, Bao Y, Zhou Y, Du F, Zhu H, Zhao S, et al. Investigation on performance and implementation of Tesla turbine in engine waste heat recovery. Energy Convers

Manag 2019;179:326–38. https://doi.org/10.1016/j.enconman.2018.10.071.

[56] Qi W, Deng Q, Chi Z, Lehao HuJiang Y, Yuan Q, Feng Z. Influence of disc tip geometry on the aerodynamic performance and flow characteristics of multichannel Tesla turbines. Energies 2019;12. https://doi.org/10.3390/en12030572.

[57] Manfrida G, Talluri L. Fluid dynamics assessment of the Tesla turbine rotor. ECOS 2016 - Proc 29th Int Conf Effic Cost, Optimisation, Simul Environ Impact Energy Syst 2016;23:1–10.

[58] Guha A, Sengupta S. A non-dimensional study of the flow through co-rotating discs and performance optimization of a Tesla disc turbine. Proc Inst Mech Eng Part A J Power Energy 2017;231:721–38. https://doi.org/10.1177/0957650917715148.

[59] Carey VP. Assessment of Tesla turbine performance for small scale rankine combined heat and power systems. J Eng Gas Turbines Power 2010;132:1–8. https://doi.org/10.1115/1.4001356.

[60] Carey VP. Assessment of Tesla Turbine Performance for Small Scale RANKINE COMBINED HEAT AND POWER SYSTEMS. Proc. ASME 2009 Int. Mech. Eng. Congr. Expo., 2009, p. 1–9.

[61] Traum MJ, Hadi F, Akbar MK. Extending “Assessment of Tesla Turbine Performance” Model for Sensitivity-Focused Experimental Design. J Energy Resour Technol Trans ASME 2018;140:1–7. https://doi.org/10.1115/1.4037967.

[62] Hoya GP, Guha A. The design of a test rig and study of the performance and efficiency of a Tesla disc turbine. Proc Inst Mech Eng Part A J Power Energy 2009;223:451–65. https://doi.org/10.1243/09576509JPE664.

[63] Qi W, Deng Q, Feng Z, Yuan Q. Influence of disc spacing distance on the aerodynamic performance and flow field of tesla turbines. Proc ASME Turbo Expo 2016;8:1–10. https://doi.org/10.1115/GT2016-57971.

[64] ABNT. NBR ISO 2768-1 Tolerâncias gerais Parte 1 : Tolerâncias para dimensões lineares e angulares sem indicação de tolerância individual. 2001.

[65] Montgomery DC. Design and analysis of simulation experiments. vol. 231. 2018.

[66] Ngo TA, Kim J, Kim SS. Characteristics of palm bark pyrolysis experiment oriented by central composite rotatable design. Energy 2014;66:7–12.

https://doi.org/10.1016/j.energy.2013.08.011.

[67] Savic IM, Savic IM, Stojiljkovic ST, Gajic DG. Modeling and optimization of energy-efficient procedures for removing lead(II) and zinc(II) ions from aqueous solutions using the central composite design. Energy 2014;77:66–72. https://doi.org/10.1016/j.energy.2014.04.088.

[68] Ait-Amir B, Pougnet P, El Hami A. Meta-model development. Embed Mechatron Syst 2015;2:151–79. https://doi.org/10.1016/b978-1-78548-014-0.50006-2.

[69] ABNT. ABNT NBR ISO 5167-1:2008. Medição de vazão de fluidos por dispositivos de pressão diferencial, inserido em condutos forçados de seção transversal circular Parte 1: Princípios e requisitos gerais. 2008.

[70] Inmetro IN de MTQ. GUM 2008 - Guia para a expressão de incerteza de medição. 2008.

[71] Coleman HW, Steele WG, Buzhuga M. Experimentation, Validation, and Uncertainty Analysis for Engineers. vol. 58. 2018. https://doi.org/10.3397/1.3383084.

[72] Ribeiro Thomazoni AL, Bazan Antequera RR, Smith Schneider P. Static Torque Measurement on a Multi Disk Turbine 2019. https://doi.org/10.26678/abcm.encit2018.cit18-0334.

[73] Dixon SL. Fluid Mechanics, Thermodynamics of Turbomachinery. 1998.

[74] Shapiro AH. The dynamics and thermodynamics of compressible fluid flow - Volume I. First. New York: The Ronald Press Company; 1953.

[75] Wakefield A. Searching and critiquing the research literature. Nurs Stand 2014;28:49–57. https://doi.org/10.7748/ns.28.39.49.e8867.

[76] Al-Ali AR, Nabulsi A Al, Mukhopadhyay S, Awal MS, Fernandes S, Ailabouni K. IoT-solar energy powered smart farm irrigation system. J Electron Sci Technol 2020;30:1–14. https://doi.org/10.1016/J.JNLEST.2020.100017.

[77] Bonjean Stanton MC, Dessai S, Paavola J. A systematic review of the impacts of climate variability and change on electricity systems in Europe. Energy 2016;109:1148–59. https://doi.org/10.1016/j.energy.2016.05.015.

[78] Liberati A, Altman DG, Tetzlaff J, Mulrow C, Gøtzsche PC, Ioannidis JPA, et al. The PRISMA statement for reporting systematic reviews and meta-analyses of studies that evaluate health care interventions: explanation and elaboration. vol. 62.

2009. https://doi.org/10.1016/j.jclinepi.2009.06.006.

[79] Tahan M, Tsoutsanis E, Muhammad M, Abdul Karim ZA. Performance-based health monitoring, diagnostics and prognostics for condition-based maintenance of gas turbines: A review. Appl Energy 2017;198:122–44. https://doi.org/10.1016/j.apenergy.2017.04.048.

[80] Liu Y, Tan L, Wang B. A review of tip clearance in propeller, pump and turbine. Energies 2018;11. https://doi.org/10.3390/en11092202.

[81] Nunes MM, Brasil Junior ACP, Oliveira TF. Systematic review of diffuser-augmented horizontal-axis turbines. Renew Sustain Energy Rev 2020;133:110075. https://doi.org/10.1016/j.rser.2020.110075.

[82] Khan KS, Kunz R, Kleijnen J, Antes G. Five steps to conducting a systematic review. J R Soc Med 2003;96:118–21. https://doi.org/10.1258/jrsm.96.3.118.

[83] Tarragona J, de Gracia A, Cabeza LF. Bibliometric analysis of smart control applications in thermal energy storage systems. A model predictive control approach. J Energy Storage 2020;32:101704. https://doi.org/10.1016/j.est.2020.101704.

[84] Eck NJ van, Waltman L. VOSviewer 2018.

[85] Song J, Ren X dong, Li X song, Gu C wei, Zhang M ming. One-dimensional model analysis and performance assessment of Tesla turbine. Appl Therm Eng 2018;134:546–54. https://doi.org/10.1016/j.applthermaleng.2018.02.019.

[86] Miller GE, Etter BD, Dorsi JM. Blood Flow Device. Ieee Trans Biomed Eng 1990;37.

[87] Adams R, Rice W. Experimental investigation of the flow between corotating disks. J Appl Mech Trans ASME 1970;37:844–9. https://doi.org/10.1115/1.3408618.

[88] Alrabie MS, Altamimi FN, Altarrgemy MH, Hadi F, Akbar MK, Traum MJ. Method To Design a Hydro Tesla Turbine for Sensitivity To Varying. ASME 2017 11th Int Conf Energy Sustain 2017:1–10.

[89] Andres JF, Loretero ME. Performance of tesla turbine using open flow water source. Int J Eng Res Technol 2019;12:2191–9.

[90] Boyack BE, Rice W. Integral Method for Flow Between Corotating Disks. J Basic Eng 1971;93:350. https://doi.org/10.1115/1.3425252.

[91] Boyd KE, Rice W. Laminar inward flow of an incompressible fluid between rotating

disks, with full peripheral admission. J Appl Mech Trans ASME 1968;36:375–7. https://doi.org/10.1115/1.3564666.

[92] Carey VP. Computational/Theoretical Modeling of Flow Physics and Transport in Disk Rotor Drag Turbine Expanders for Green Energy Conversion Technologies. Proc. ASME 2010 Int. Mech. Eng. Congr. Expo., 2010, p. 31–8. https://doi.org/10.1115/imece2010-41017.

[93] Chen J, Tang W, Han K, Xu L, Chen B, Jiang T, et al. Bladeless-Turbine-Based Triboelectric Nanogenerator for Fluid Energy Harvesting and Self-Powered Fluid Gauge. Adv Mater Technol 2019;4:1–7. https://doi.org/10.1002/admt.201800560.

[94] Choon TW, Rahman. AA, Jer FS, Aik LE. Optimization of Tesla turbine using computational fluid dynamics approach. 2011 IEEE Symp Ind Electron Appl ISIEA 2011 2011:477–80. https://doi.org/10.1109/ISIEA.2011.6108756.

[95] Choon TW, Anasrahman A, Li TS. Tesla Turbine for Energy Conversion 2012:820–5.

[96] Ciappi L, Fiaschi D, Niknam PH, Talluri L. Computational investigation of the flow inside a Tesla turbine rotor. Energy 2019;173:207–17. https://doi.org/10.1016/j.energy.2019.01.158.

[97] Cilingir AC. Design , Manufacturing and Testing of a Hybrid Tesla Turbine. Int J Eng Adv Technol 2019;8:267–70.

[98] Crowell R. Generation of Electricity Utilizing Solar Hot Water Collectors. Proc. ASME 2009 3rd Int. Conf. Energy Sustain., 2009, p. 1–8.

[99] Engelbrecht EG, Giakoumis Z, Sidiropoulos S, Chasoglou A, Chokani N. Modelling phase change in a novel turbo expander for application to heat pumps and refrigeration cycles. E3S Web Conf 2019;113:1–7. https://doi.org/10.1051/e3sconf/201911303012.

[100] Fiaschi D, Talluri L. Design and off-design analysis of a Tesla Turbine utilizing CO2 as working fluid. E3S Web Conf 2019;113:1–6. https://doi.org/10.1051/e3sconf/201911303008.

[101] Garrison PW, Harvey DW, Catton I. Laminar Compressible Flow Between Rotating Disks. J Fluids Eng 1976;98:382. https://doi.org/10.1115/1.3448330.

[102] Guha A, Smiley B. Experiment and analysis for an improved design of the inlet and

nozzle in Tesla disc turbines. Proc Inst Mech Eng Part A J Power Energy 2010;224:261–77. https://doi.org/10.1243/09576509JPE818.

[103] Guha A, Sengupta S. The fluid dynamics of the rotating flow in a Tesla disc turbine. Eur J Mech B/Fluids 2013;37:112–23. https://doi.org/10.1016/j.euromechflu.2012.08.001.

[104] Guha A, Sengupta S. The fluid dynamics of work transfer in the non-uniform viscous rotating flow within a Tesla disc turbomachine. Phys Fluids 2014;26. https://doi.org/10.1063/1.4866263.

[105] Jonsson M, Zurbuchen A, Haeberlin A, Pfenniger A, Vogel R. Vascular turbine powering a cardiac pacemaker: An in-vivo case study. Exp Clin Cardiol 2014;20:2000–3. https://doi.org/10.7892/boris.48128.

[106] Khan MUS, Ali E, Maqsood MI, Nawaz H. Modern improved and effective design of boundary layer turbine for robust control and efficient production of green energy. J Phys Conf Ser 2013;439. https://doi.org/10.1088/1742-6596/439/1/012043.

[107] Khan MUS, Maqsood MI, Ali E, Jamal S, Javed M. Proposed applications with implementation techniques of the upcoming renewable energy resource, the Tesla Turbine. J Phys Conf Ser 2013;439. https://doi.org/10.1088/1742-6596/439/1/012040.

[108] Mandal A, Saha S. Performance analysis of a centimeter scale Tesla turbine for micro-air vehicles. Proc Int Conf Electron Commun Aerosp Technol ICECA 2017 2017;2017-Janua:62–7. https://doi.org/10.1109/ICECA.2017.8203625.

[109] Manfrida G, Pacini L, Talluri L. A revised Tesla Turbine Concept for ORC applications. Energy Procedia 2017;129:1055–62. https://doi.org/10.1016/j.egypro.2017.09.115.

[110] Neckel AL, Godinho M. Influence of geometry on the efficiency of convergent-divergent nozzles applied to Tesla turbines. Exp Therm Fluid Sci 2015;62:131–40. https://doi.org/10.1016/j.expthermflusci.2014.12.007.

[111] Papagianni A, Efstathiadis T, Gaitanis A, Kalfas A. Modelling of a Tesla turbine gap between the rotor disks. E3S Web Conf 2019;113:2–3. https://doi.org/10.1051/e3sconf/201911303013.

[112] Pater LL, Crowther E, Rice W. Flow Regime Definition for Flow Between Corotating

Disks 1974.

[113] Paweł BAGIŃSKI, Łukasz JĘDRZEJEWSKI2. THE STRENGTH AND DYNAMIC ANALYSIS OF THE PROTOTYPE OF TESLA TURBINE 2015.

[114] Reich A, Deaconu S. Development and testing of a small scale bladeless turbine for power production applications. ASME Int Mech Eng Congr Expo Proc 2009;1:59–65. https://doi.org/10.1115/IMECE2009-12373.

[115] Romanin VD, Carey VP. An integral perturbation model of flow and momentum transport in rotating microchannels with smooth or microstructured wall surfaces. Phys Fluids 2011;23. https://doi.org/10.1063/1.3624599.

[116] Schosser C, Klingl S, Lecheler S, Fuchs T, Hain R, Kähler C, et al. Comprehensive investigation of the flow in a narrow gap between co-rotating disks. Eur J Mech B/Fluids 2019;78:50–61. https://doi.org/10.1016/j.euromechflu.2019.05.014.

[117] Sengupta S, Guha A. Analytical and computational solutions for three-dimensional flow-field and relative pathlines for the rotating flow in a Tesla disc turbine. Comput Fluids 2013;88:344–53. https://doi.org/10.1016/j.compfluid.2013.09.008.

[118] Sengupta S, Guha A. Flow of a nanofluid in the microspacing within co-rotating discs of a Tesla turbine. Appl Math Model 2016;40:485–99. https://doi.org/10.1016/j.apm.2015.05.012.

[119] Shah V, Dhokai S, Patel P. Bladeless turbine - A review. Int J Mech Eng Technol 2017;8:232–6.

[120] Sheikhnejad Y, Simões J, Martins N. Energy harvesting by a novel substitution for expansion valves: Special focus on city gate stations of high-pressure natural gas pipelines. Energies 2020;13. https://doi.org/10.3390/en13040956.

[121] Siddiqui MS, Ahmed H, Ahmed S. Numerical Simulation of a Compressed Air Driven Tesla Turbine. Proc. ASME 2014 Power Conf., 2014, p. V002T09A009. https://doi.org/10.1115/power2014-32069.

[122] Song J, Gu CW. 1-D model analysis of Tesla Turbine for small scale Organic Rankine Cycle (ORC) system. Proc ASME Turbo Expo 2017;3:1–10. https://doi.org/10.1115/GT2017-63797.

[123] Talluri L, Fiaschi D, Neri G, Ciappi L. Design and optimization of a Tesla turbine for ORC applications. Appl Energy 2018;226:300–19.

https://doi.org/10.1016/j.apenergy.2018.05.057.

[124] Traum MJ, Weiss HL. Tiny Tesla Turbine Analytical Performance Validation Via Dynamic Dynamometry. E3S Web Conf 2019;113:1–8. https://doi.org/10.1051/e3sconf/201911303024.

[125] Valente A. Installation for pressure reduction of hydrocarbon gases in a near isothermal manner. Soc Pet Eng - 13th Abu Dhabi Int Pet Exhib Conf ADIPEC 2008 2008;2:1187–93. https://doi.org/10.2118/118034-ms.

APPENDIX

Systematic literature review

Traditional Literature Reviews (TLR) basically summarize. critically analyze. evaluate. and clarify ideas that have been presented by other researchers. a Systematic Literature Review (SLR) develop: (i) an article search strategy in order to ensure that all the relevant articles are included; (ii) a strict inclusion and exclusion criteria is established; and (iii) a template for data entry. using a well- defined categories and coding schemes with a view to produce an unbiased outcome. [75,76]. The SLR is a structured form of conducting a literature review. aiming to reach comprehensive and reliable results to answer a specific well-delineated research question. however. it is not properly explored by many other disciplines. including engineering. even if it is a well-known technique widely adopted in several different research areas such as medical and human sciences [77]. A systematic review must present a clear and reproducible methodology. always keeping the target of including all the relevant studies in the field of interest. As stated by [78]. managing the bias risk is one of the most important objectives of a SLR. Lately. engineering studies. some of them related to turbines and pumps. have been adopting SLR to map the field of research. previous discoveries. and to support their conclusions [79–81].Thus. aiming to better understand the landscape and map the state-of-the-art of the Tesla turbine research field. a comprehensive literature review was conducted in which some procedures and techniques from a SRL were adopted. observing the recommendations from [82]. A systematic review protocol was used to register all the steps of the review process. such as: (i) article selection process; (ii) bibliometric and scientometric analysis; and (iii) content analysis.

Bibliometric analysis

Bibliometric analysis is a powerful tool to summarize large amounts of scientific data ([83]). In this paper a bibliometric and a scientometric analysis were carried out to identify the most prominent authors and research groups in the field. as well as the most relevant works. the evolution in time of the used keywords and expressions. The entire set of works resulted from the previous section (**Error! Reference source not found.**)

was analyzed in the VOSWiewer software [84]. and the following analyses were carried out: i) keyword co-occurrence. ii) citation per document. iii) citation per author.

The authors believe that the spread of publications in this research field is intimately related to two world trends: (i) the search for innovative. highly efficient energy solutions in a sustainable world; (ii) the increase in the use of Computation Fluid Dynamics (CFD) to analyze and solve problems that involve fluid flows. which is corroborated by the analysis presented in the following sections.

Figure A.1 shows that the map of the most frequent words adopted among the analyzed works. The two most frequent keywords *turbines* and *tesla turbine* were removed for the sake of clarity. In addition. all the expressions containing the keyword *efficiency* were merged to better represent its predominance compared to other keywords.

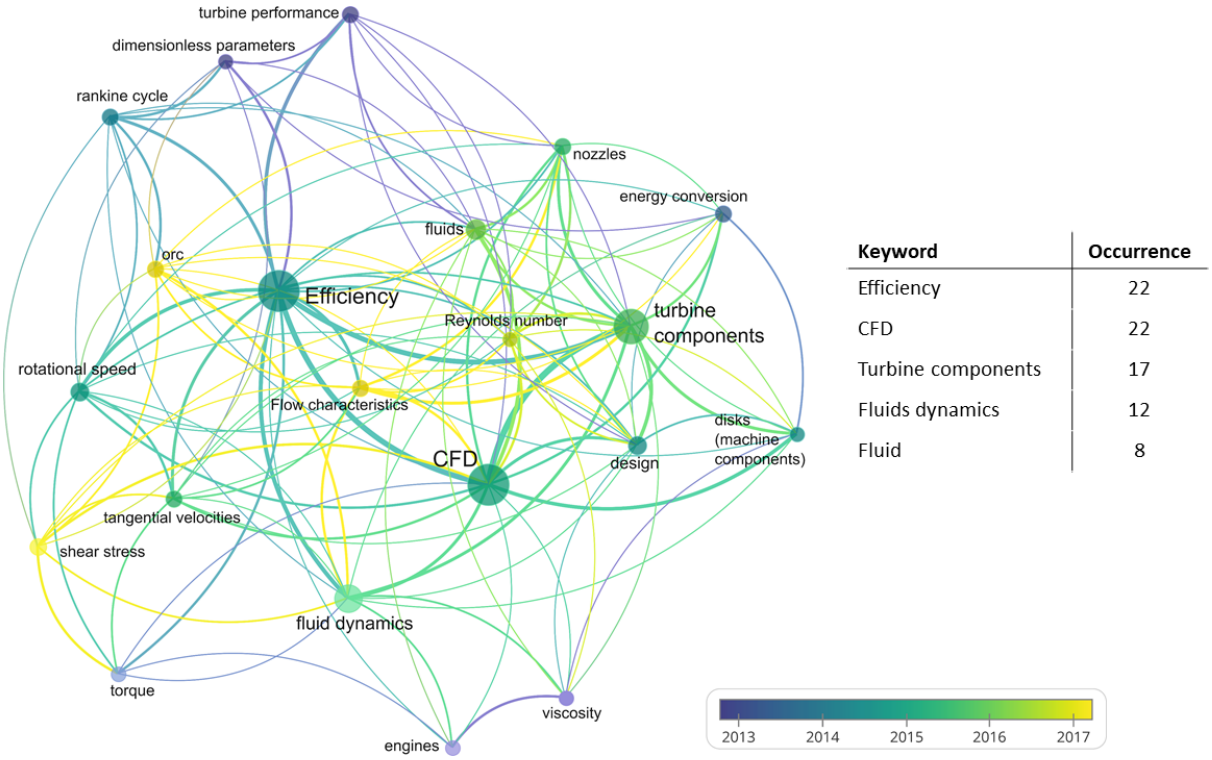

Keyword	Occurrence
Efficiency	22
CFD	22
Turbine components	17
Fluids dynamics	12
Fluid	8

Figure A.1 – Map of keyword co-occurrence. The circle size represents the number of keyword occurrences and colors are related to the time.

The terms “Efficiency” and “CFD” are both the most frequent keywords. The presence of “Efficiency” indicates that it is the main turbine performance parameter and a current point of interest in Tesla turbines studies. The expression “CFD” can be related

to the recent developments in CFD tools. allowing for more detailed and complex analysis of fluid flow and energy transfer related phenomena. In third place is “Turbine components”. which is associated with researchers approaches that discretize the turbine in their components to identify separately its performances and efficiencies. The map also indicates that most recent studies deal with Organic Rankine Cycle (ORC). which corroborates with the Tesla turbine relation with recent energy generation and recovery studies. Finally. it is worth noticing that the time range in the map legend is relatively short (2012-2018). since the large part (78 of 86) of the studies were published after year 2000.

The author citation map is presented in Figure A.2. The most cited paper is the one from [3]. which is a high-quality experimental and analytical work that served as reference for several subsequent publications. The paper received 72 citations.

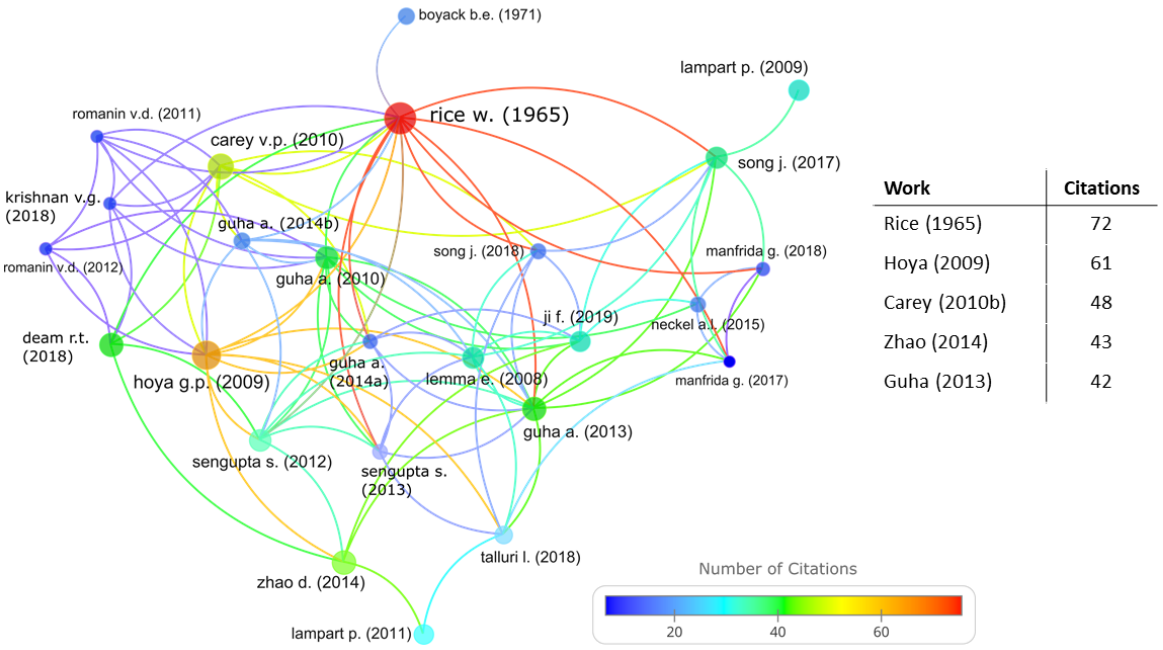

Work	Citations
Rice (1965)	72
Hoya (2009)	61
Carey (2010b)	48
Zhao (2014)	43
Guha (2013)	42

Figure A.2 – Map of citation per document. Circle size and colors represent the number of occurrences.

The second most cited paper (61 citations). is another experimental work of [62] followed by the analytical exploration of the tesla turbine presented by [59] with 48 citations. The most prominent authors in the field are shown in Figure A.3. Professor Abhijit Guha from the Indian Institute of Technology Kharagpur is the most cited author

having been cited 240 times for his works in Tesla turbines. Sayantan Sengupta is the second most cited author (140 citations). followed by Carey V.P. with 98 citations.

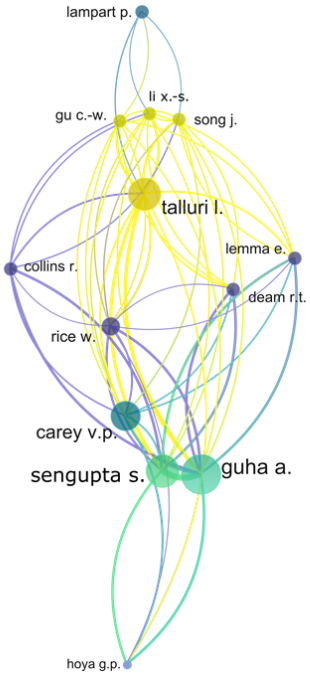

Author	Documents	Citations
Guha A.	9	240
Sengupta S.	7	140
Carey V.P.	6	98
Rice W.	3	92
Collins R. Deam R.T Lemma E.	2	74

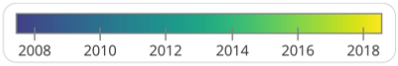

Figure A.3 – Map of citation per author. Circle size means the number of published works.

An interesting finding refers to the international collaboration network on Tesla turbine publications. Figure A.4. As observed in. there are several isolated research groups around the globe. However. despite their internal connections of co-authorship. there is not a wide co-authorship collaboration between the research groups. and consequently. between different countries. This tendency resulted in several groups working independently. which may have influenced the developments on Tesla turbine research.

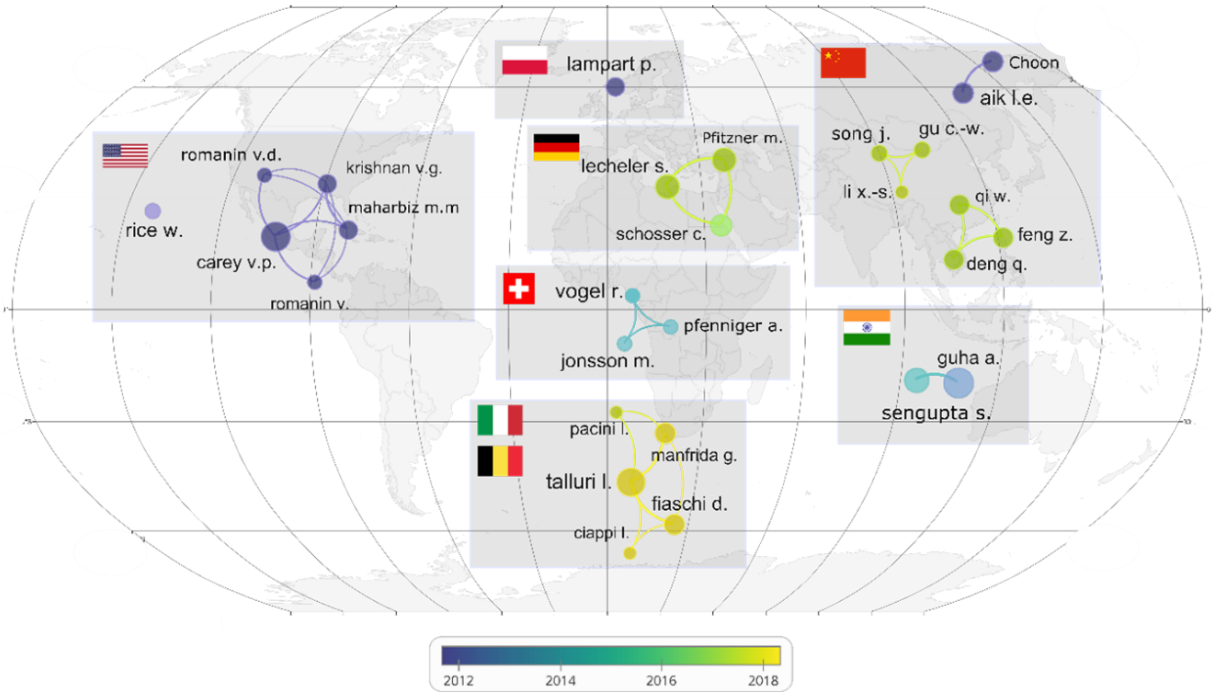

Figure A.4 – Map of co-authorship and respective country. Colors relate to the average publication year. and circle sizes indicate the number of published works of each author.

Additional information of the content analysis

Tesla Turbine applications

The Tesla turbine potential uses were identified in a timeline. Figure A.5. together with the total number of occurrences that an application was recommended.

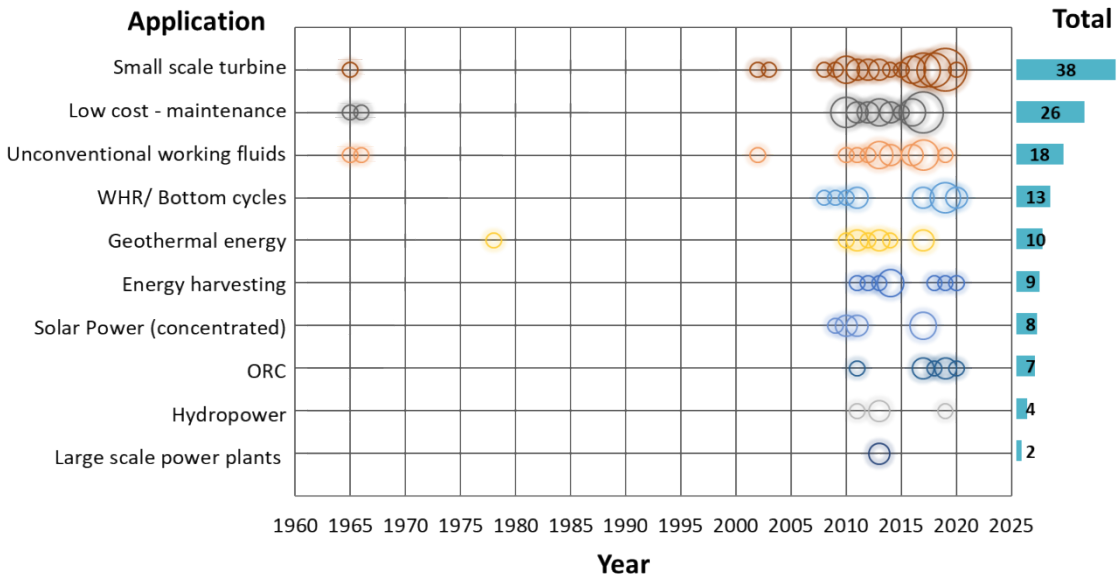

Figure A.5 – Timeline for reported TT applications. The circle diameter indicates the number of reported applications by year.

From Figure A.5. it can be observed that the most relevant application is to use Tesla as a small-scale turbine. This is corroborated by the findings exposed in Figure 3. that presents the larger part of the research with output power lower than 20 kW. The small-scale turbine category is closely related to other listed ones as energy harvesting. waste heat recovery (WHR)/ bottom cycle. and Organic Rankine Cycle (ORC). which can be seen as more specific applications for Tesla turbine. For the ORC applications. recently interesting works were published in which Tesla turbine was analyzed as expanders in ORC [2,7,8,43,44,85]. The second most reported application is the use of Tesla turbines as a low-cost/maintenance turbine. Nevertheless. we didn't find studies comparing the Tesla turbine to other small-scale expanders. The third most suggested application is the use of unconventional working fluids. which is assessed through identifying the reported working fluids in Tesla turbine research. Figure A.6 . Other applications were also found. but they were suppressed from Figure A.6 due to their lower occurrence.

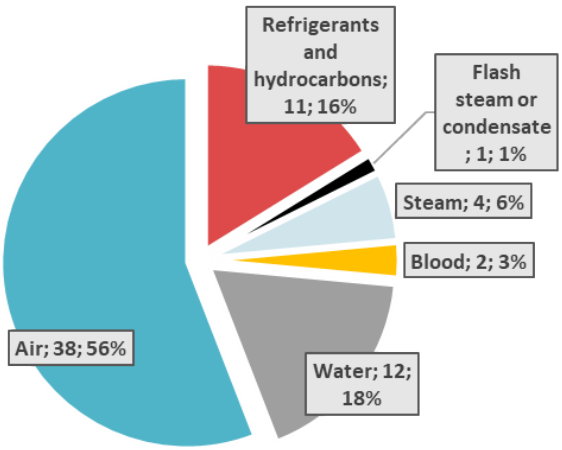

Figure A.6 – Working fluids utilized in Tesla turbines.

Figure A.6. shows that the largest part of the studies (56%) utilized air as working fluid. due to its easy availability. managing. and conditioning. Water and hydrocarbons/refrigerants are the second and third most used work fluids. respectively. This last one presented an increase due to recent developments in ORC studies. An interesting application for the Tesla turbine was reported in [33,86]. in which it served as an energy recovery device. installed in bloodstreams to power up equipment like a

pacemaker. It was also found studies that analyzed Tesla turbines running with steam and flash steam. however. none of them presented experimental approaches.

Tesla Turbine output power and efficiency time-based evolution

Figure A.7 presents a timeline for reporting efficiency in research articles. It makes a distinction between experimental and not experimental approaches (hatched areas). and the y-axis presents the number of published works considering the ranges of output power and efficiency. From the timeline presented in Figure A.7. it is possible to see that for most of the recent works (2002 to 2020) the number of experimental approaches is 44%. Finally. taking into account the whole timeframe (1965 to 2020) is possible to conclude that no clear evolution in efficiency values is observed.

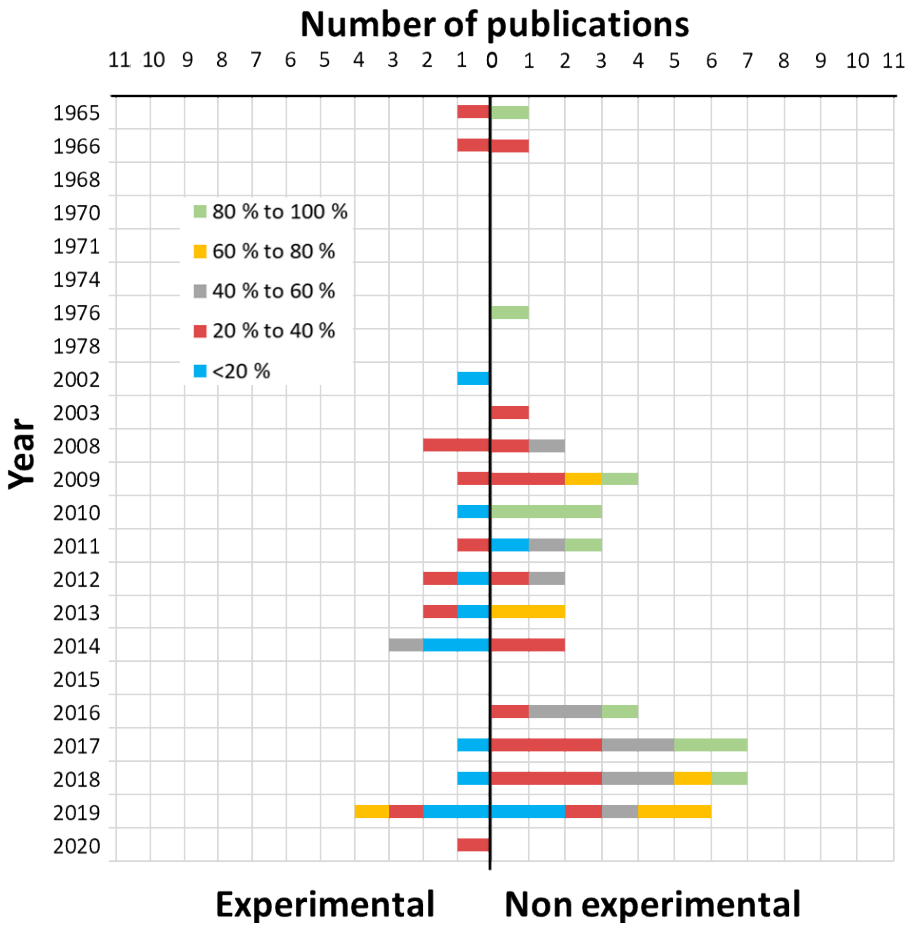

Figure A.7 – Timeline of reported efficiency.

Figure A.8 presents a timeline for reported output power. It indicates that recent reports of non-experimental output power (from 2002) have been largely focused on small-scale developments. lower than 1 kW. It is worth noticing that reports on sub-watt scale Tesla turbine began in 2016. along with energy harvesting topics. Reported output power for experimental works. shows a decreasing behavior. from the medium power range (1 kW to 20 kW) reaching the lower ones (<1 kW). This trend can be interpreted as an attempt to size down Tesla turbines to obtain higher efficiencies. which is the same trend observed for the non-experimental output power.

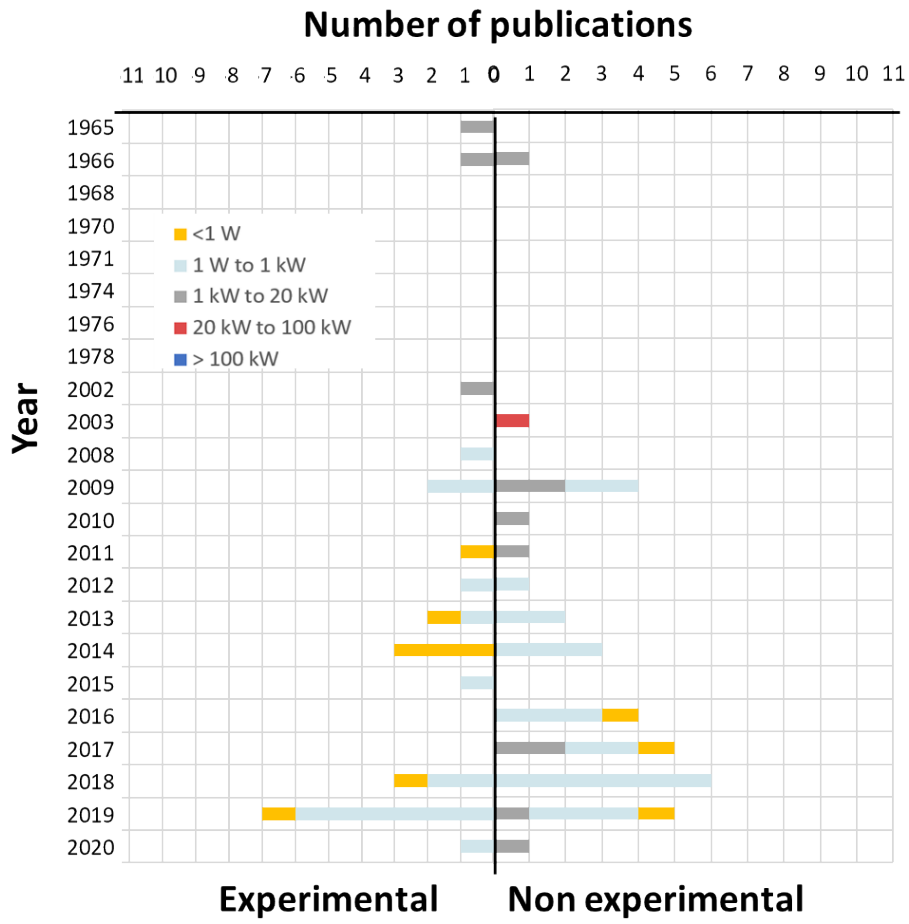

Figure A.8 – Timeline of reported output power.

Critical review

The SLR results pointed out Tesla turbine characteristics such as key parameters classification (independent variables). performance map (reported efficiency and power

output). and its most common applications. The analysis of independent variables shows that more than 16 different types of modifiable parameters in the TT field. For these variables. no quantitative or qualitative ranking considering the effects of changes in independent variables. like those obtained during the DoE analysis. was found. Also. different trends were observed on the effects in output power and efficiency for some independent variables.

Reported efficiency values in nonexperimental studies ranged from 40% to 60%. on average. The average efficiency reported by experimental studies was just above 20%. which points out the lack of consensus regarding the TT maximum efficiency. Probably. higher efficiency could be found for generated power ≤ 1 kW and forward into sub-Watt scale. However. is still to be proven if its performance can be competitive concerning other turbine technologies.

The analysis of TT applications shows that this equipment is mainly reported as a small-scale turbine and its other described strong points are yet to be validated. Among Tesla turbine reported experimental approaches. only three used “non-conventional” fluids. which demonstrate that this TT characteristic is still to be proved. In addition. as far as the authors are aware. no published work suggests that Tesla turbines are a low-cost and/or low-maintenance alternative.

These findings indicate that experiments which present a ranking of independent parameters cause-effect magnitude and statistical ground are fundamental to further development in this research field. An extra benefit of the DoE methodology application is a higher standardization in the analysis since it was shown that in many studies the determination of TT efficiency does not present technical rigor.

It is interesting to highlight that Tesla turbines are expected to present higher output power values for higher rotational speeds. However. this behavior is obtained considering an increase in the available turbine inlet energy or a decrease in rotor outer diameter. which leads to lower turbine efficiencies. Therefore. this characteristic combined with the findings presented in Figure 3 and Figure A.5. reinforces that the spectrum of application for Tesla turbine is restricted to small scale turbines (output power <1 kW). and to the subWatt scale.

Table A.1 – Considered works in SLR.

Work	Pub. year	Type of study				Efficiency range					
		Review	Experimental	CFD	Analytical	<20	20-40	40-60	60-80	80-100	Not reported
[87]	1970		X								X
[88]	2017				X						
[89]	2019		X				X				
[4]	1966			X							
[48]	2012		X		X		X				
[90]	1971		X			X					
[91]	1968				X						
[60]	2009				X						
[92]	2010				X						
[59]	2010				X						
[93]	2019				X						
[94]	2011		X	X							X
[95]	2012		X	X	X						X
[96]	2019		X	X							X
[97]	2019			X	X						
[98]	2009		X								X
[50]	2008				X						
[51]	2013		X		X		X				
[99]	2019			X	X						
[100]	2019			X							
[101]	1976				X						
[102]	2010				X						
[103]	2013		X	X							X
[104]	2014				X						
[25]	2014			X	X						
[58]	2017			X	X						
[52]	2016			X							
[62]	2009			X							
[27]	2019		X				X				
[105]	2014		X	X							X
[54]	2019		X			X					
[106]	2013		X						X		
[107]	2013		X								X
[28]	2019				X						
[29]	2011			X	X						
[12]	2013		X				X				
[45]	2009		X		X		X				
[46]	2011			X							
[30]	2008			X							

Table A.1(cont.) – Considered works in SLR.

Work	Pub. year	Type of study				Efficiency range					
		Review	Experimental	CFD	Analytical	<20	20-40	40-60	60-80	80-100	Not reported
[31]	2003		X	X			X				
[32]	2017				X						
[108]	2017		X	X	X	X					
[57]	2016			X	X						
[109]	2017				X						
[7]	2018				X						
[110]	2015				X						
[111]	2019		X		X						X
[53]	2002			X							
[112]	1974		X			X					
[113]	2015		X								X
[33]	2014		X	X				X			
[63]	2016			X							
[34]	2018			X							
[35]	2018			X							
[56]	2019			X							
[114]	2009		X		X						X
[3].	1965		X		X		X				
[49]	2010		X		X	X					
[115]	2011				X						
[11]	2012		X	X	X		X				
[36]	2018		X	X		X					
[37]	2018		X	X							X
[38]	2019		X	X	X	X					
[47]	2019		X			X					
[39]	2014		X	X							X
[40]	2017			X	X						
[116]	2019		X	X	X						X
[23]	2012				X						
[117]	2013			X	X						
[118]	2016			X	X						
[21]	2017	X									
[119]	2017		X								X
[41]	2013		X			X					
[120]	2020			X							
[121]	2014			X							
[122]	2017				X						
[8]	2017				X						
[85]	2018				X						
[123]	2018			X	X						
[44]	2020		X				X				

Table A.1(cont.) – Considered works in SLR.

Work	Pub. year	Type of study				Efficiency range					
		Review	Experimental	CFD	Analytical	<20	20-40	40-60	60-80	80-100	Not reported
[61]	2019				X						
[124]	2018		X		X						X
[5]	1976				X						
[125]	2008		X								X
[10]	2014		X	X		X					
[22]	2019	X									

Test rig information

Table A.2 – Test rig components.

TAG	Description	Model	Range	Sensitivity	Sensor datasheet uncertainty
-	Compressor	BRAVO CSL 60BR/350	-	-	-
PI01	Pressure indicator	-	0-17 bar	0.1 bar	-
VE01	Valve	-	-	-	-
PCV01	Pressure control valve	Norgren R17	0.3 – 8.5 bar	-	-
TI01	Temperature indicator	-	0-200 °C	5 °C	-
-	Heater	Electric resistance	-		-
TT01	Temperature transmitter - CLP	PT-100 – NOVUS	0-300 °C	380 mΩ/°C	± 0.55 °C
VE02	Valve	-	-	-	-
VE03	Valve	-	-	-	-
PT01	Pressure transmitter (gauge) – Inlet	PS-10B	0-10 bar	46 mV/kPa	± 0.05 bar
TT02	Temperature transmitter – Inlet	Thermocouple K	-200 to 1250 °C	41 µV/°C	± 0.5 °C
PT02	Pressure transmitter (gauge) – Housing	PSE550-X505	- 0.5 bar-g to + 0.5 bar-g	46 mV/kPa	± 0.005 bar
TT03	Temperature transmitter - Housing	Thermocouple K	-200 to 1250 °C	41 µV/°C	± 0.5 °C
LC01	Load cell	Bonad - Bnd - Ic5.0	0 – 1 [kg]	1 mV/V	± 0.005 [kg]
SS01	Speed sensor	BR200DDTN	-	-	-
PT03	Pressure transmitter (gauge) – Outlet	PSE550-X505	- 0.5 bar-g to + 0.5 bar-g	46 mV/kPa	± 0.005 bar
TT04	Temperature transmitter – Outlet	Thermocouple K		41 µV/°C	± 0.5 °C
-	Venturi	-	-		-
DPT01	Differential pressure transmitter – Venturi	MPXV7002	-2 to 2 kPa	1 V/kPa	± 50 Pa
TT05	Temperature transmitter - Environment	-	-	41 µV/°C	± 0.5 °C
	Heater CLP	NOVUS 1000	-	-	-
	Auto transformer	Varivolt 1.6 kVA	-	-	-

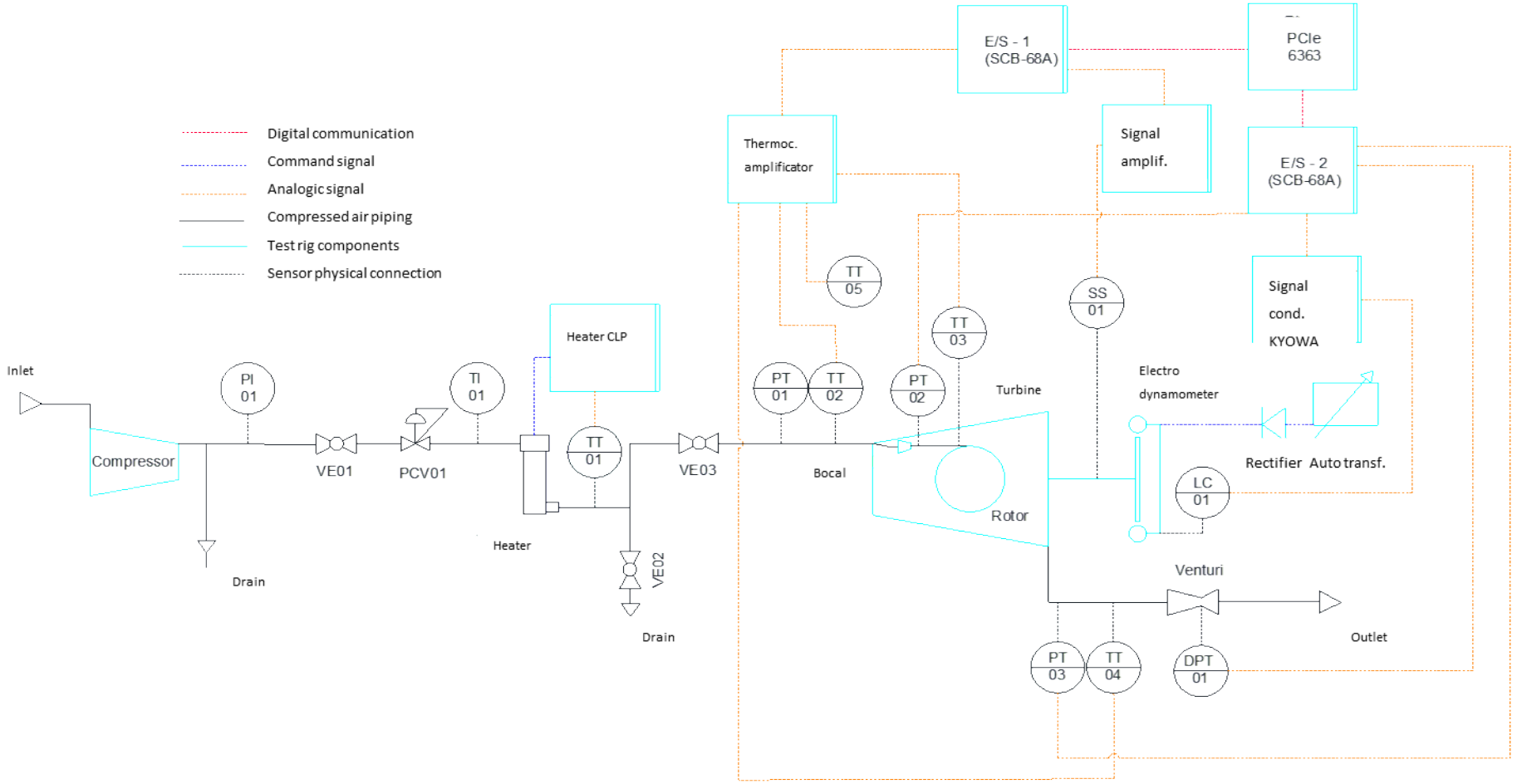

Figure A.9 – Test rig systematic drawing.

Database

Table A.3 – Mean values for independent and dependent variables for CCD – database.

Essay order	Rotational speed [rpm]	T_{turb} [Nm]	$\dot{W}_{turb}$ [W]	Inlet temp. [C]	Housing temp. [C]	Outlet temp. [C]	Environment temp. [C]	Inlet pres. [bar-g]	Housing pres. [bar-g]	Outlet pres. [bar-g]	$\dot{m}_V$ [kg/s]	η_{m-turb} [%]
1	4008	0.93	390	39.0	28.2	23.9	22.6	2.99	-0.093	-0.118	0.0254	14.0
2	4005	0.71	298	30.4	22.3	23.3	22.6	2.49	-0.101	-0.121	0.0226	13.3
3	4011	0.70	294	50.2	36.5	29.7	22.6	2.49	-0.106	-0.123	0.0216	12.9
4	4013	0.73	307	39.3	28.7	23.5	22.4	2.49	-0.098	-0.118	0.0220	13.7
5	4009	0.45	189	40.8	33.4	29.3	22.8	2.00	-0.112	-0.127	0.0187	10.8
6	4011	0.72	302	39.7	30.9	30.8	22.7	2.50	-0.106	-0.124	0.0222	13.3
7	3999	0.71	297	40.1	29.5	28.5	22.6	2.49	-0.109	-0.127	0.0220	13.2
8	6024	0.05	32	30.8	29.1	27.2	22.6	2.00	-0.084	-0.129	0.0193	1.9
9	2018	0.68	144	50.2	35.9	30.0	21.9	1.99	0.005	-0.001	0.0182	8.2
10	6001	0.40	251	29.6	22.3	22.7	22.3	3.01	-0.090	-0.139	0.0265	9.3
11	4007	0.75	315	40.3	26.9	22.7	21.3	2.49	-0.121	-0.139	0.0220	13.8
12	2013	1.01	213	40.1	29.7	24.8	21.4	2.49	-0.143	-0.139	0.0222	9.3
13	4007	0.75	315	40.3	26.9	22.7	21.3	2.49	-0.121	-0.139	0.0220	13.8
14	5995	0.05	31	50.2	36.7	28.5	22.1	2.00	-0.090	-0.132	0.0183	1.7
15	5998	0.24	151	39.9	36.7	34.0	22.5	2.49	-0.075	-0.125	0.0218	6.7
16	1996	0.63	132	30.1	26.0	26.7	22.0	1.99	-0.131	-0.126	0.0195	7.5
17	5982	0.42	263	50.2	37.7	28.2	22.2	2.99	-0.071	-0.126	0.0248	9.3
18	2022	1.23	260	30.0	23.8	24.5	22.2	3.00	-0.128	-0.128	0.0261	9.3
19	4016	0.75	315	39.4	33.8	30.5	22.4	2.49	-0.109	-0.128	0.0222	13.9
20	2012	1.24	261	50.6	38.1	30.1	22.0	2.99	-0.129	-0.129	0.0251	9.1

Table A.3 (cont.) – Mean values for independent and dependent variables for CCD – database.

Essay order	Rotational speed [rpm]	T_{turb} [Nm]	$\dot{W}_{turb}$ [W]	Inlet temp. [C]	Housing temp. [C]	Outlet temp. [C]	Environment temp. [C]	Inlet pres. [bar-g]	Housing pres. [bar-g]	Outlet pres. [bar-g]	$\dot{m}_V$ [kg/s]	η_{m-turb} [%]
21	4000	0.94	394	40.2	29.7	29.6	22.9	2.99	-0.105	-0.129	0.0250	14.2
22	4019	0.69	290	29.9	24.6	25.5	22.7	2.50	-0.109	-0.130	0.0226	12.9
23	4010	0.73	307	50.3	36.6	29.2	22.3	2.50	-0.112	-0.131	0.0218	13.2
24	3991	0.72	301	39.9	34.4	31.2	22.9	2.49	-0.112	-0.131	0.0222	13.2
25	4001	0.43	180	39.6	29.5	29.5	22.8	1.99	-0.117	-0.131	0.0192	10.0
26	3985	0.69	288	40.2	29.1	27.8	22.7	2.49	-0.113	-0.131	0.0223	12.5
27	4009	0.73	306	40.4	27.9	25.9	23.0	2.49	-0.110	-0.131	0.0233	12.8
28	6027	0.05	32	30.3	27.1	24.4	25.2	2.00	-0.095	-0.141	0.0208	1.6
29	2001	0.68	142	50.5	34.8	29.1	25.3	2.00	-0.182	-0.175	0.0196	7.2
30	5996	0.43	270	30.1	25.3	29.3	25.1	2.99	-0.047	-0.107	0.0267	9.6
31	3993	0.76	318	40.9	28.0	24.9	24.6	2.49	0.033	-0.005	0.0234	13.4
32	1995	1.00	209	39.9	32.7	29.1	24.8	2.49	0.003	-0.008	0.0226	9.0
33	3996	0.74	310	41.0	29.7	26.6	25.0	2.49	0.032	-0.006	0.0227	13.2
34	6025	0.06	38	49.9	38.1	30.3	24.0	2.00	0.051	-0.012	0.0193	2.0
35	6012	0.24	151	39.3	37.4	33.0	24.0	2.49	0.052	-0.018	0.0229	6.5
36	1999	0.64	134	29.6	26.9	28.0	24.0	2.00	-0.126	-0.122	0.0207	7.2
37	5985	0.44	276	49.4	36.5	25.3	23.7	3.01	-0.068	-0.124	0.0269	9.0
38	2001	1.25	262	29.6	24.6	25.8	23.9	2.99	-0.120	-0.121	0.0268	9.2
39	4014	0.76	319	40.0	27.0	22.2	23.6	2.51	-0.103	-0.123	0.0230	13.6
40	2006	1.26	265	49.7	34.5	29.1	23.8	2.99	-0.127	-0.127	0.0260	9.5

Table A.4 – Essays by order: measured value vs predicted value.

Essay Order	Measured value				Predicted value			
	$\dot{m}_V$ [kg/s]	T_{turb} [Nm]	[W]	$\dot{W}_{turb}$ [%]	$\dot{m}_V$ [kg/s]	T_{turb} [Nm]	[W]	$\dot{W}_{turb}$ [%]
1	0.0254	0.93	390	14	0.0257	0.93	383	14.6
2	0.0226	0.71	298	13.3	0.0229	0.72	302	13.3
3	0.0216	0.7	294	12.9	0.0219	0.72	302	13.3
4	0.022	0.73	307	13.7	0.0225	0.72	302	13.3
5	0.0187	0.45	189	10.8	0.0192	0.45	200	10.2
6	0.0222	0.72	302	13.3	0.0225	0.72	304	13.3
7	0.022	0.71	297	13.2	0.0224	0.72	302	13.3
8	0.0193	0.05	32	1.9	0.0197	0.04	25	2
9	0.0182	0.68	144	8.2	0.0186	0.65	135	7.6
10	0.0265	0.4	251	9.3	0.0264	0.42	268	9.4
11	0.022	0.75	315	13.8	0.0224	0.72	302	13.3
12	0.0222	1.01	213	9.3	0.0224	0.98	211	9.4
13	0.022	0.75	315	13.8	0.0224	0.72	302	13.3
14	0.0183	0.05	31	1.7	0.0187	0.04	29	2.1
15	0.0218	0.24	151	6.7	0.0224	0.26	157	6.6
16	0.0195	0.63	132	7.5	0.0197	0.65	133	7.5
17	0.0248	0.42	263	9.3	0.0252	0.42	266	9.4
18	0.0261	1.23	260	9.3	0.0263	1.25	267	9.2
19	0.0222	0.75	315	13.9	0.0225	0.72	302	13.3
20	0.0251	1.24	261	9.1	0.0251	1.24	265	9.2
21	0.025	0.94	394	14.2	0.0257	0.93	383	14.6
22	0.0226	0.69	290	12.9	0.023	0.72	304	13.3
23	0.0218	0.73	307	13.2	0.022	0.72	304	13.3
24	0.0222	0.72	301	13.2	0.0224	0.72	302	13.3
25	0.0192	0.43	180	10	0.0192	0.44	198	10.1
26	0.0223	0.69	288	12.5	0.0224	0.72	302	13.3
27	0.0233	0.73	306	12.8	0.0224	0.72	302	13.3
28	0.0208	0.05	32	1.6	0.0197	0.04	25	1.9
29	0.0196	0.68	142	7.2	0.0187	0.66	135	7.6
30	0.0267	0.43	270	9.6	0.0262	0.42	265	9.3
31	0.0234	0.76	318	13.4	0.0224	0.72	302	13.3
32	0.0226	1	209	9	0.0224	0.98	209	9.3
33	0.0227	0.74	310	13.2	0.0224	0.72	302	13.3
34	0.0193	0.06	38	2	0.0187	0.04	25	1.9
35	0.0229	0.24	151	6.5	0.0225	0.26	155	6.5
36	0.0207	0.64	134	7.2	0.0197	0.66	135	7.6
37	0.0269	0.44	276	9	0.0253	0.42	270	9.5
38	0.0268	1.25	262	9.2	0.0262	1.25	264	9.1
39	0.023	0.76	319	13.6	0.0226	0.73	306	13.4
40	0.026	1.26	265	9.5	0.0252	1.24	264	9.2